

Article

A Computer Tool for Modelling CO₂ Emissions in Driving Tests for Vehicles with Diesel Engines

Karol Tucki 

Department of Production Engineering, Institute of Mechanical Engineering, Warsaw University of Life Sciences, Nowoursynowska Street 164, 02-787 Warsaw, Poland; karol_tucki@sggw.edu.pl; Tel.: +48-593-45-78

Abstract: The dynamic development of transport in recent decades reflects the level of economic development in the world. The transport sector today is one of the main barriers to the achievement of the European Union's climate protection objectives. More and more restrictive legal regulations define permissible emission limits for the amounts of toxic substances emitted into the atmosphere. Numerical CO₂ modeling tools are one way to replace costly on-road testing. Driving cycles, which are an approximation of the vehicle's on-road operating conditions, are the basis of any vehicle approval procedure. The paper presents a computer tool that uses neural networks to simulate driving tests. Data obtained from tests on the Mercedes E350 chassis dynamometer were used for the construction of the neural model. All the collected operational parameters of the vehicle, which are the input data for the built model, were used to create simulation control runs for driving tests: Environmental Protection Agency, Supplemental Federal Test Procedure, Highway Fuel Economy Driving Schedule, Federal Test Procedure, New European Driving Cycle, Random Cycle Low, Random Cycle High, Mobile Air Conditioning Test Procedure, Common Artemis Driving Cycles, Worldwide Harmonized Light-Duty Vehicle Test Procedure. Using the developed computer simulation tool, the impact on CO₂ emissions was analyzed in the context of driving tests of four types of fuels: Diesel, Fatty Acid Methyl Esters, rapeseed oil, butanol (butyl alcohol). As a result of the processing of this same computer tool, mass consumption of fuels and CO₂ emissions were analyzed in driving tests for the given analyzed vehicle.



Citation: Tucki, K. A Computer Tool for Modelling CO₂ Emissions in Driving Tests for Vehicles with Diesel Engines. *Energies* **2021**, *14*, 266. <https://doi.org/10.3390/en14020266>

Received: 14 December 2020
Accepted: 4 January 2021
Published: 6 January 2021

Publisher's Note: MDPI stays neutral with regard to jurisdictional claims in published maps and institutional affiliations.



Copyright: © 2021 by the author. Licensee MDPI, Basel, Switzerland. This article is an open access article distributed under the terms and conditions of the Creative Commons Attribution (CC BY) license (<https://creativecommons.org/licenses/by/4.0/>).

Keywords: computer simulation; vehicle; engine; biofuel; neural network

1. Introduction

The list below contains a set of the most important quantities used in the calculations with the appropriate symbols and units (Table 1). The table below also lists the most important abbreviations used in the manuscript.

The main idea conveyed in the concept of sustainable transport is to minimize the harmful impact of transport means on the environment—both natural and that of large urban agglomerations [1–3]. Taking into account the fact that the number of vehicles travelling on roads increases every year, air pollution also increases [4–6]. It is the composition of the air-fuel mixture [7–10] that is one of the most important factors that affect the content level of the three most dangerous substances in exhaust gases, i.e., carbon dioxide, hydrocarbons, and nitrogen oxides. The automotive industry is facing enormous challenges [11–15]. Market forecasts show that although combustion-engine cars are being ousted by vehicles with electric motors, they are still leading in the sales results of large automotive corporations [16–19]. As internal combustion engines have a huge share among the emitters of pollutants to the atmosphere, a downward trend can be observed for the volumes of diesel cars, which are being replaced by electric, petrol, and hybrid cars [20–22]. These tendencies result from increasingly restrictive exhaust emission standards [23–25]. The lowered exhaust emission limits are a challenge for motor designers and significantly influence the development of internal combustion engines and their accessories. An addi-

tional issue is the migration of car brands in the world and the standards that cars must meet in a given region of the world [26–30].

Table 1. Abbreviations, symbols and units used in the manuscript.

Symbol	Description	Unit
EPA	Environmental Protection Agency	
FTP	Federal Test Procedure	
SFTP	Supplemental Federal Test Procedure	
HWFET	Highway Fuel Economy Test Driving Schedule	
MAC TP	Mobile Air Conditioning Test Procedure	
NEDC	New European Driving Cycle	
CADC	Common Artemis Driving Cycles	
WLTP	Worldwide Harmonized Light-Duty Vehicle Test Procedure	
FAME	Fatty Acid Methyl Esters	
ARTEMIS	Assessment and Reliability of Transport Emission Models and Inventory Systems	
UDC	Urban Driving Cycle	
EUDC	Extra Urban Driving Cycle	
EU	European Union	
RDE	Real Driving Emissions	
WLTC	Worldwide Harmonized Light-Duty Vehicles Test Cycles	
PSA	Peugeot Société Anonyme	
FCA	Fiat Chrysler Automobiles	
VECTO	Vehicle Energy Consumption Calculation Tool	
HDV	Heavy Duty Vehicles	
ASTM	American Society for Testing and Material	
n_{engine}	Engine rotational speed for the given gear number	min^{-1}
v_{vehicle}	Vehicle speed for the given gear number	km/h
x_i	Input signals for the neuron	
w_i, u_i, v_i	Weight values of neurons in individual layers	
b_i	Polarity values of neurons in individual layers	
y_i	Given learning values	
d_i	Values of network responses in the learning process	
n_{engine}	Measured value of the engine rotational speed	min^{-1}
Fuel	Measured value of the fuel flow	g/s
Fuel_i real cycle	Mass of fuel consumed in the i th real road test carried out by EPA (tests: US 06, US highway, FTP 75)	kg
Fuel_i simul cycle	Mass of fuel consumed in the i th road test from the developed simulation (tests: US 06, US highway, FTP 75)	kg
T_{engine}	The torque produced by the motor	$\text{N}\cdot\text{m}$
Cal_i	Calorific value for i fuel	J/kg
w_i	Mass fraction of i th fuel in the mixture	kg/kg
$\text{Cal}_{\text{Diesel}}$	Calorific value for diesel fuel	J/kg
Cal	Calorific value for other fuel	J/kg
C_i	Mass fraction of carbon in i th fuel	kg/kg
w_i	Mass fraction of i th fuel in the mixture	kg/kg

In its transport policy, the European Union has been trying for many years to find a compromise between environmental, economic, and social priorities [31–34]. Vehicle emissions to the atmosphere are controlled by increasingly stringent standards [35,36]. The introduced regulations allow to control the amount of emitted substances and are an impulse for the development of low emission technologies [37–40].

The driving cycle is used to measure fuel consumption and CO_2 and pollutant emissions from passenger cars and light commercial vehicles in a standardized manner [41,42]. Currently, from a regulatory point of view, it is the only standardized way to analyze the amount of pollutant emissions from vehicles. For this type of testing, chassis test bench (a roller dynamometer station) are used. During the test, the exhaust gases are taken from the vehicle's exhaust pipe. The emission factors are then evaluated [43,44]. In the case of commercial vehicles, only tests of the engine alone with the power transmission

system are applied on an engine dynamometer [45,46]. A set of engine torque and speed points are used for driving cycle analysis [47,48]. Modal tests are used (e.g., NEDC—New European Driving Cycle) and transient driving cycles (e.g. FTP75—Federal Test Procedure, ARTEMIS—Assessment and Reliability of Transport Emission Models and Inventory Systems). Modal cycles, as opposed to transition cycles, are defined by a set of accelerations and constant velocities [49,50].

The driving tests and emission standards introduced concern new passenger cars. They are subject to obligatory type-approval tests, including the determination of road emissions of the vehicle [51,52]. Fuel consumption and pollutant emissions are affected by, *inter alia*, driving patterns, traffic conditions, and weather conditions, which vary from one geographical region to another. This makes it necessary to differentiate between the existing driving tests worldwide [53,54]. The procedures in place take into account the use of on-board systems (e.g., air conditioning) and urban and non-urban driving patterns [55,56]. These cycles are mostly intended for light vehicles, passenger cars, and those intended for heavy goods vehicles contain only information about engine operation times at a given load [57–61].

In 1992, fuel consumption and exhaust emissions in the EU for light vehicles (with a reference mass not exceeding 2610 kg) were measured using the New European Driving Cycle that consisted of the UDC (Urban Driving Cycle) and the EUDC (Extra Urban Driving Cycle) [62–64]. In the urban cycle, the car was accelerated (on the rollers of the dynamometer) to an average speed of about 18 kph and the maximum speed did not exceed 50 kph. In the extra-urban cycle, the average speed was about 62 kph, and the maximum speed was 120 kph, or 90 kph in the case of low capacity vehicles [65,66]. In the case of the NEDC standard, the exhaust gas analysis was performed according to the constant volume technique with the use of special measuring equipment [67–69].

Laboratory conditions turned out to be unsuitable for calculating the real values of fuel consumption and exhaust emissions. Therefore, from September 2018, all exhaust emissions of all new cars sold in the EU are measured according to the WLTP (Worldwide Harmonized Light Vehicles Test Procedure) and RDE (Real Driving Emissions) standards [70–74]. The WLTP was responsible for measurements in laboratory conditions, and RDE for measurements of harmful substances directly on the road [75,76].

The WLTP uses the new Worldwide Harmonized Light-Duty Vehicles Test Cycles to measure fuel consumption, CO₂ emissions and pollutant emissions from passenger cars and light commercial vehicles. It provides more realistic data, which better reflects the daily use of the vehicle [77,78].

In the case of the WLTP standard, four speed ranges are measured on the dynamometer after a cold start: up to 60 kph, up to 80 kph, up to 100 kph and above 130 kph. Within each phase, accelerations and decelerations occur. The top speed is 10 kph higher than that of the NEDC. The entire WLTP cycle takes approximately 30 min and the distance covered is 23 km. Unlike the NEDC procedure, the WLTP takes into account additional accessories that may affect weight, aerodynamics and electric energy consumption (idle current) [79,80].

The MAC TP (Mobile Air Conditioning Test Procedure) cycle test procedure is used to measure any additional fuel consumption and pollutant emissions caused by the operation of the mobile air conditioning system (MAC) in a passenger car. The procedure was developed for the needs of the European Commission in 2010 and involves physical testing of the whole vehicle on a chassis dynamometer in an emission laboratory. The MAC test cycle has a total of 6 phases [81,82].

The CADC (Common Artemis Driving Cycles) includes measurement procedures performed on a chassis dynamometer, developed on the basis of real on-road runs by ARTEMIS [83–85]. The CADC consists of three driving cycles: urban, extra-urban, and motorway. The motorway test is divided into two variants: with maximum speeds of 130 and 150 kph. Artemis driving cycles assume appropriate gearshift sequences on the test

vehicle [86–88]. The study was based on a statistical analysis of a database of real European driving patterns [89,90].

In the USA, exhaust emissions from passenger cars and light trucks with diesel engines are determined for a given vehicle in accordance with the Supplementary Federal Test Procedure (SFTP) [91,92]. The SFTP consists of three test cycles: part of the FTP-75 (Federal Test Procedure) chassis dynamometer cycle, the SFTP US06 aggressive high speed driving cycle, and the SFTP SC03 high ambient temperature tests with air conditioning load [93–95]. The main feature of the FTP-75 cycle is the 17.77 km distance that the car must cover in 1874 s, with an average speed of 34.1 kph [96,97]. In turn, the SC03 procedure involves testing the vehicle on a chassis dynamometer at an ambient temperature of 35 °C in order to determine the emissions from the vehicle with the air conditioning device turned on inside it. The vehicle covers the distance of 5.8 km [98,99] with an average speed of 34.8 kph within the 595 s of the test duration. The US06 SFTP procedure was developed to supplement the FTP-75 test with car drive simulation (duration 595 s) in a more dynamic manner (12.8 km distance) and at a higher speed (average speed 77.9 kph, top speed 129.2 kph) [100–102]. The HWFET (Highway Federal Extra Test) developed by the US EPA (United States Environmental Protection Agency) is used to assess fuel consumption. The entire test lasts 765 s, during which the vehicle covers a distance of 16.45 km, with an average speed of 77.7 kph [103–105].

Last year, the maximum permissible average emission intensity of cars sold in the EU was still 130 gCO₂/km. Manufacturers did meet these requirements without any problems (by reaching as low as 123 gCO₂/km) [106,107]. On 1 January 2020, new regulations on exhaust emission standards for new passenger cars came into force in the European Union. Initially, only new cars (with a new type-approval) will have to comply with the new standards, and from 2021 all vehicles sold will have to comply. The aim of those standards is to eliminate cars emitting more than 95 g/km of CO₂. This means that each passenger car will not be able to burn more than 3.5 liters of fuel for every hundred kilometers travelled. These will be the most stringent limits in the world. For comparison, in 2021 the US will have a limit of 125 gCO₂/km, Japan will have 122 gCO₂/km, and China 117 gCO₂/km [108]. Diesel engines, on the other hand, will be completely banned from passenger cars.

The above-mentioned goal is slightly different for each of the automakers—Daimler, which traditionally produces larger and heavier cars, must meet the limit of 103 gCO₂/km, BMW has a 2 g lower limit, while concerns like PSA (Peugeot Société Anonyme) (including Peugeot) and FCA (Fiat Chrysler Automobiles) (e.g., Fiat), which traditionally produce smaller cars, cannot exceed 91 gCO₂/km.

Just two years ago, the EU decided to take the next steps—lowering the emission targets for 2021 by 15% by 2025 and by 37.5% by 2030. If MEPs and member states follow the Commission's proposal, the 2030 target will be tightened to a 50% reduction compared to the 2021 target, which would mean an average of 42.5 gCO₂/km in 2030.

From the point of view of CO₂ emissions, the use of biofuels is also important [109,110].

In Polish climatic conditions, the main source of plant esters is rapeseed oil [111]. The high cetane number theoretically allows it to be used directly as a fuel for diesel engines. However, the modern diesel engine has been designed and improved for combustion of mineral diesel fuel, which has different physicochemical properties. The use of crude rapeseed oil (a mixture of triacylglycerols) requires a special adjustment of injection systems and combustion chambers [112].

For many years, methyl esters of higher fatty acids (FAME) have also been used to reduce the consumption of fuels from non-renewable sources in motor vehicles [113,114]. This kind of fuel is used in the form of a few percent solutions with conventional fuel or as a standalone B100 fuel. Higher fatty acid methyl esters (FAME) are mainly obtained from oils from various oil plants. However, both for environmental protection and economic improvement purposes, used vegetable oils and some animal fats are also used in the production of higher fatty acid methyl esters (FAME). Like conventional fuel, FAME is

characterized by a tendency to solidify (crystallize) at low temperatures. This process causes the fuel to lose its fluidity and become solidified.

Decreasing reserves of crude oil, increasing consumption of liquid fuels used in transport, and increasing emissions of harmful components of exhaust gases into the atmosphere force an intensive search for alternative sources of energy to be used in road transport. Apart from bioethanol and rapeseed oil methyl esters, research is being carried out on the possibilities of producing fuels from biomass (biobutanol), waste, and non-food agricultural products of other bio-components. Biobutanol is obtained by anaerobic fermentation similar to that of ethanol, but with the use of different microorganisms in the process. Butanol is more energy-efficient than ethanol because it contains more carbon. This alcohol can be obtained from by-products of the food industry and the pulp and paper industry [115,116].

It should be emphasized that commonly used biocomponents such as bioethanol and fatty acid methyl esters (FAME) are called first generation biofuels. According to the EU policy, the emphasis in recent years has been placed on the development of new technologies for the conversion of inedible and waste materials to second-generation biofuels (e.g., from lignocellulosic waste) as well as third-generation biofuels from raw materials derived from dedicated biological processes [117,118].

An example of a tool introduced by the European Commission to calculate CO₂ emissions and fuel consumption of HDVs (Heavy Duty Vehicles) is the VECTO (Vehicle Energy Consumption Calculation Tool) simulation program [119]. The developed program uses the results of measurements of the vehicle's components influencing energy consumption (the input data) and the results of the vehicle simulation under different driving conditions [120]. Parameters constituting the input data of the program are, among others: aerodynamic resistance, engine performance, torque losses in the powertrain, engine fuel map, axle and transmission efficiency, power demand of auxiliary equipment, tire rolling resistance. VECTO computes the fuel consumption in liters per 100 kilometers and the fuel consumption per transported tonne kilometer, as well as the CO₂ emissions.

The manuscript [121] proposes an integrated methodology for estimating bus emissions from the fleet of vehicles of the Municipal Transport Company in Madrid. The proposed solution uses both measured transport activity data and vehicle activity data with specific emission models to calculate consumption and emissions for the bus fleet in an urban area.

In the manuscript [122] biharmonic maps were used to predict the emission of NO_x (nitrogen oxides) and the relative fuel-air ratio of a city bus. The instrumented city bus has been tested during actual passenger transport. The experimental results were consistent with biharmonic maps predictions. Important parameters for prediction of NO_x concentration were vehicle speed and relative fuel-air ratio.

The aim of the paper was to build a computer tool that uses neural networks to simulate drive tests. The constructed driving test simulator determines the amount of CO₂ emissions and fuel demand for given input parameters and fuel type. There were 12 drive tests analyzed in the paper, which are valid in different parts of the world.

2. Materials and Methods

As part of the project, a quantitative model of specific fuel consumption was prepared as a function of rotational speed and torque of a diesel engine, based on data published by EPA. Error backpropagation neural networks with the Levenberg–Marquardt learning algorithm were used to build the quantitative model. Then, the input data for the driving tests were prepared using the “Gearshift Calculation Tool” programme for the selected vehicle [123].

The above activities were necessary to simulate the operation of the selected vehicle in driving tests, in order to obtain the amount of CO₂ emissions and fuel demand for the fuels used (diesel oil, FAME, rapeseed oil, and butanol).

Table 2 below summarizes the basic properties of the fuels used [124–126].

Table 2. Basic properties of fuels used in computer simulation.

Property	Test Methods	Diesel	FAME	Rapeseed Oil	Butanol
Carbon content [%]		86.5	78.0	77.4	64.8
Hydrogen content [%]		13.4	12.0	11.4	13.5
Oxygen content [%]		0.0	10.0	11.2	21.6
Air demand [g_{air}/g_{fuel}]		14.5	12.5	12.5	11.2
Lower heating value [MJ/kg]	ASTM D-240	44.0	37.1	37.5	33.0
Cinematic viscosity at 40 °C [mm^2/s]	ASTM D-445	2.8	3.8	36	3.6
Particulate matter content [mg/kg]	DIN 51419	24	25	<25	22
Ash content [mg/kg]	DIN ISO 6245	0.01	0.01	<0.01	0.01
Sulphur content [mg/kg]	ASTM D5453	10	6.5	10	10
Water content [mg/kg]	ASTM D1744	190	500	<1000	500
Phosphorus content [mg/kg]	DIN 51 363T1	-	8.7	12	0.2

2.1. The Vehicle Used in Driving Tests

The development of the simulation model for driving tests was based on the 2013 Mercedes E350 BlueTEC vehicle research [127]. Table 3 below presents the most important technical parameters of the vehicle and the factors necessary to be used in driving tests and programs generating the required runs: vehicle speed, gear number, clutch engagement, and pedal position.

Table 3. Parameters of the vehicle used in the tests for drive tests.

Parameter	Description	Unit
Vehicle (MY, Make, Model)	2013 Mercedes E350	-
Equivalent test mass	2041	kg
Rated power (declared)	195	kW
Rated engine speed (declared)	3800	min^{-1}
Idling engine speed (declared)	600	min^{-1}
Max vehicle speed(declared)	250	km/h
Number of gears	7	-
Ratio n/v_1, gear 1	87.72	h/(km·min)
Ratio n/v_2, gear 2	57.47	h/(km·min)
Ratio n/v_3, gear 3	38.61	h/(km·min)
Ratio n/v_4, gear 4	27.47	h/(km·min)
Ratio n/v_5, gear 5	20.08	h/(km·min)
Ratio n/v_6, gear 6	16.47	h/(km·min)
Ratio n/v_7, gear 7	14.62	h/(km·min)
Target Coeff f0	161.9	N
Target Coeff f1	0.8485	N/(km/h)
Target Coeff f2	0.02696	N/(km/h) ²

The values of the Ratio n/v coefficient for individual gears were calculated on the basis of the relationship allowing for data contained in [128]:

$$\text{Ratio } n/v = n_{\text{engine}}/v_{\text{vehicle}} \text{ [h/(km}\cdot\text{min)}] \quad (1)$$

2.2. Neural Networks

The structures of the “Multilayer Feedforward Backpropagation Network” neural network with approximating properties were used to build the neural model. The structure of the neural network included non-linear activating functions $f_1(x)$ and $f_2(x)$ determined by the dependencies in the hidden layers, and the output layer included a linear activating function $f_3(x)$ in the form:

$$f_1(x) = \frac{2}{1 + \exp(-2 \sum_{i=1}^n w_i x_i + b_i)} \quad (2)$$

$$f_2(x) = \frac{2}{1 + \exp(-2 \sum_{i=1}^n u_i x_i + b_i)} \quad (3)$$

$$f_3(x) = \sum_{i=1}^n v_i x_i + b_i \quad (4)$$

The network learning process employed the Levenberg–Marquardt algorithm whose basis is the optimization process by finding the minimum value of the objective function defined as the mean value of the sum of squared differences between the current values of the network output signals and the set values in the form:

$$\Delta \bar{e}^2 = \frac{1}{m} \sum_{i=1}^m (d_i - y_i)^2 \quad (5)$$

Figure 1 shows a general schematic of the neural network structure that meets the above dependencies. The “Neural Network Module Version 3.0” library in the Scilab 6.1.0 numerical software [129,130] was used to build the neural model.

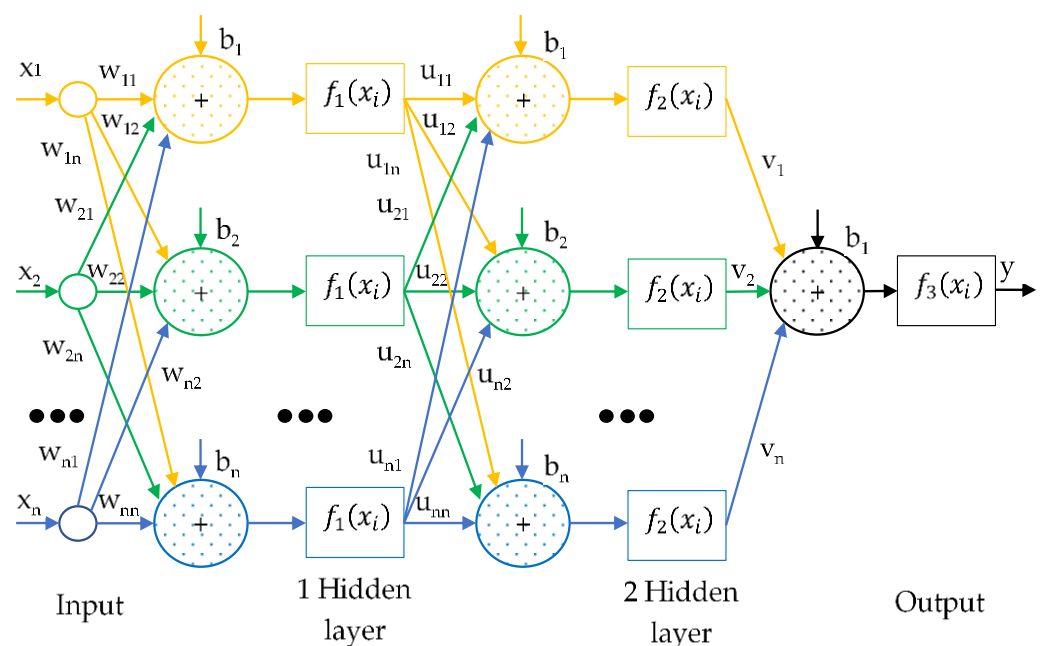


Figure 1. General schematic of the applied structure of the neural network.

2.3. Data for Building the Neural Model

The published data obtained during the 2013 Mercedes E350 vehicle tests on a chassis dynamometer were used in the building of the neural model that enables the calculation of the instantaneous value of the fuel flow as functions of: engine rotational speed, engine-generated torque, gear number in the transmission, and vehicle speed [127]. In order to remove from the measurement data the influence of rotational speed on the data values, further calculations used the parameter of the amount of injected fuel per 1 work cycle, which was calculated on the basis of the dependence:

$$\text{Fuel}_{\text{cycle}} = \text{Fuel} \cdot 0.12 / n_{\text{engine}} \text{ [kg/cycle]} \quad (6)$$

Figure 2 shows the set of points obtained during vehicle tests on a chassis dynamometer, converted to the value of the amount of injected fuel per one injection cycle.

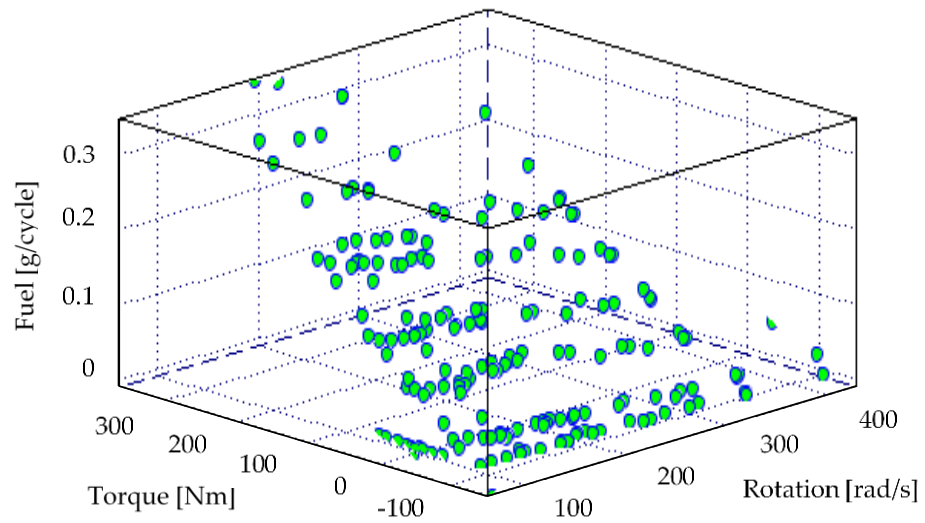


Figure 2. Fuel consumption measurement points for one fuel injection cycle as a function of engine rotational speed and engine torque used for the construction of the neural model.

2.4. Optimization of the Selection of the Structure of the Neural Network

In order to obtain a neural model characterized by the best degree of adjustment to the research data published by EPA [127], a process of optimizing the selection of the neural network structure was carried out, taking into account the change in the number of input parameters: engine speed, engine torque, vehicle gear number, vehicle speed, and change the number of hidden neurons. In the optimization process, a scalar objective function was used in accordance with the dependence:

$$\text{minimum} \left(\frac{\sum_{i=1}^n | \text{Fuel}_i \text{ real cycle} - \text{Fuel}_i \text{ simul cycle} |}{\sum_{i=1}^n \text{Fuel}_i \text{ real cycle}} \right) \text{ [kg]} \quad (7)$$

Figure 3 presents selected results of the optimization process for various tested network structures which differ in the number of input parameters and the number of neurons in the hidden layer, and which obtained the greatest degree of matching to the research data in many iterations.

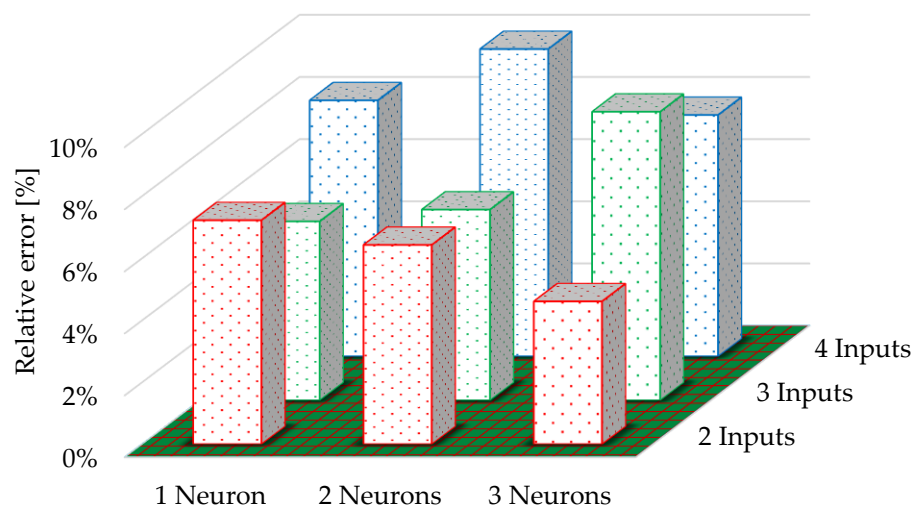


Figure 3. Summary of learning results for the best-adjusted neural networks for the characteristic of specific fuel consumption. The calculated relative error between the model and actual data: 2 inputs: engine rotational speed, engine torque; 3rd input: vehicle gear number; 4th input: vehicle speed.

The relative error was 4.7% for the selected neural network structure.

For the further stages of building a vehicle simulation in road tests, it was decided to select a neural network structure with two inputs for the input signals: engine rotational speed, engine torque, and 3 neurons in the hidden layer.

2.5. Theoretical Assumptions of the Model

The published test results on the chassis dynamometer were achieved using standard, commercially available diesel fuel. The assumptions of the work done on the simulation of the vehicle in driving tests included the introduction of a functionality that enabled the determination of the consumption of other fuels used to power diesel engines. It is with the use of the neural model, on the basis of the instantaneous values of the engine-generated torque and the engine rotational speed, that the instantaneous values of the fuel stream for diesel are obtained from the dependence:

$$\dot{Fuel}_{Diesel} = f_{Net}(n_{engine}, T_{engine}) \text{ [kg/s]} \quad (8)$$

Then, the calorific value is calculated in the simulation, in the case of using a fuel other than diesel or mixtures thereof, from the dependence:

$$Cal = \sum_{i=1}^n w_i \cdot Cal_i \text{ [J/kg]} \quad (9)$$

The calculations assumed that, for the instantaneous load resulting from the rotational engine speed and the engine-generated torque, a stream of another fuel must provide the same amount of energy over time as in the case of diesel, and the efficiency of operation in the case of an engine powered by other fuels is the same as for diesel fuel, for a given calculation point. In this case, the instantaneous stream of fuels other than diesel is calculated from the dependence:

$$Fuel = Fuel_{Diesel} \frac{Cal_{Diesel}}{Cal} \text{ [kg/s]} \quad (10)$$

Figure 4 presents the flow of the instantaneous values of the specific fuel consumption as a function of the engine rotational speed and the engine-generated torque for 4 types of fuels used in the simulation (diesel, FAME, rapeseed oil, butanol).

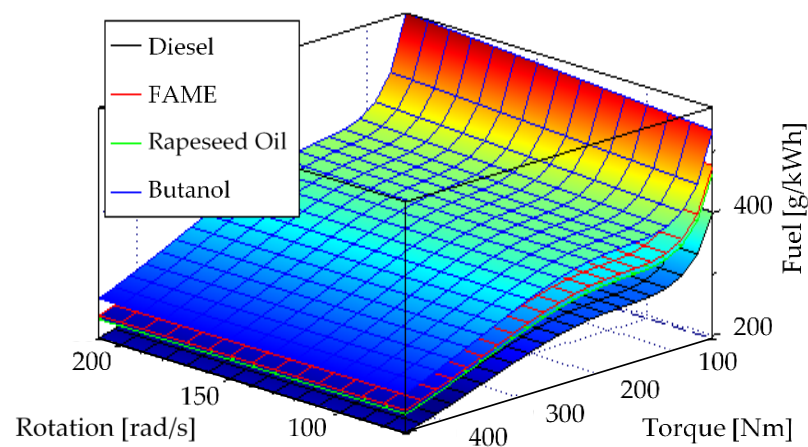


Figure 4. Model of specific fuel consumption characteristics built with the use of a neural network and used in further simulations.

For the calculation of carbon dioxide emissivity, it was possible to calculate the mass content of carbon in the analyzed fuel, based on the available information on the chemical compositions of the individual components of the mixture, the mass content of the fuel

in the mixture and the instantaneous fuel stream resulting from the engine operating conditions using the dependence:

$$\dot{C}O_2 = 3.664 \cdot \text{Fuel} \cdot \sum_{i=1}^n w_i \cdot C_i \text{ [kg/s]} \quad (11)$$

2.6. Driving Test Generator

Based on the collected data of operational parameters of the vehicle in question and using the “Gearshift calculation tool” [123] application, runs for simulation control were created for the following drive tests:

- US 06—The US06 (SFTP) [131,132]
- US highway—Highway Fuel Economy Driving Schedule (HWFET) [133,134]
- FTP 75—EPA Federal Test Procedure [135,136]
- NEDC—New European Driving Cycle (NEDC) [137,138]
- US SC03—The SC03 (SFTP) [139,140]
- Random Cycle Low (x05)—a test generated from a procedure in the WLTP Random Cycle Generator tool [141,142]
- Random Cycle High (x95)—a test generated from a procedure in the WLTP Random Cycle Generator tool [143,144]
- MAC TP cycle—mobile air conditioning (MAC) [145]
- CADC—Artemis cycle definitions, includes the following cycles: Urban, Rural Road, Motorway [146,147]
- CADC without MOT (Motorway) —Artemis cycle definitions, includes the following cycles: Urban, Rural Road. Does not include: Motorway [146,147]
- CADC abridged—Same as Artemis cycle definitions, includes the following cycles: Urban, Rural Road, Motorway. The duration time has been shortened, similar to CADC without MOT [146,147]
- WLTC 3b random (Worldwide Harmonized Light-duty Vehicles Test Cycles) —WLTP for class 3 vehicles with the engine power above 34 W/kg [41,148].

After the complete information about the vehicle has been entered, the program enables the generation of the necessary waveforms in the time domain, which enable the determination of the instantaneous operating parameters of the analyzed programme. Then, these waveforms were exported to the Excel file format. For further stages of the simulation, the instantaneous waveforms of the following quantities were used: simulation time [s]; engine rotational speed [rpm]; power generated by the engine [kW]; torque generated by the engine [Nm]—a value calculated on the basis of engine rotational speed and engine power; gear number [-]; vehicle speed [kph].

2.7. Simulator

Based on the analysis of the data created with the use of the “Gearshift Calculation Tool” programme, the results of the process of optimization of the neural network structures and the properties of the biofuels in question, a driving test simulator was developed in Scilab 6.1.0. The simulator consists of blocks responsible for individual functionalities, whose connection schematic is presented in Figure 5:

- Driving test generator from Excel files—responsible for loading files with data controlling the selected driving test process from the spreadsheet created with the use of the “Gearshift Calculation Tool” programme and for converting the read data to formats compatible with Scilab 6.1.0. The following parameters are transferred to the calculation modules of the simulation: engine speed, engine torque, vehicle speed, simulation time;
- Model of specific Diesel consumption (neural)—this block calculates the instantaneous values of Diesel mass flow and transfers this parameter to the next block, based on the quantities characterizing the engine’s operating parameters: engine speed, engine torque and the prepared neural network structure;

- Calculations of fuel and CO₂ mass flows—this block is responsible for calculating the streams of the biofuels in question necessary to power the engine in the driving test, using the diesel mass flow parameter and the fuel calorific value characteristic for the given fuel in question, calculated in the previous block. This block also calculates the carbon dioxide emission stream using the carbon mass content in the fuel and the instantaneous fuel stream;
- Calculation of driving test parameters—on the basis of the driving test parameters, this block calculates the distance travelled by the vehicle during the test, the power generated by the engine and the mechanical energy generated during the test.

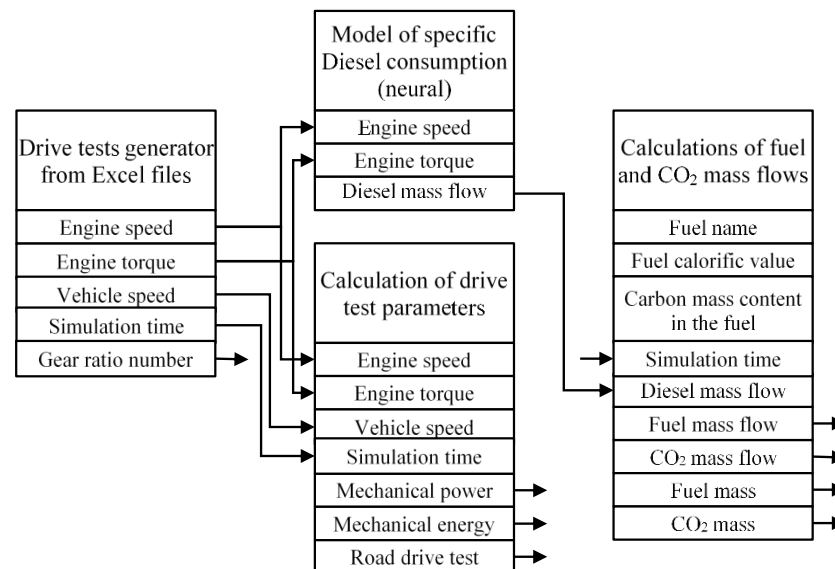


Figure 5. General schematic of the driving tests, including biofuels.

3. Results

The following are the processes of independent simulations of a selected 2013 Mercedes E350 vehicle in the applied driving tests with fuels changing (Diesel, FAME, rapeseed oil, butanol):

- the results of the simulation work for the processed data from EPA tests, which are learning models for the neural network
- the results of the driving test simulator for the prepared drive tests (the “Gearshift Calculation Tool” programme) in the form of graphs of the vehicle speed, distance travelled, engine rotational speed, engine torque, engine power, and mechanical energy consumed during the test
- the simulation results for the stream and final fuel consumption
- the simulation results for the stream and carbon dioxide emissions for selected driving tests and selected fuels for the 2013 Mercedes E350 vehicle
- the results of the fuel consumption and CO₂ emissivity per 1 km of the distance travelled by the vehicle in the tests and per 1 kWh of the generated mechanical energy power in the test.

3.1. Simulation Work Results for Processed EPA Test

In order to verify the correct operation of the drive test simulator, the published data were used from actual vehicle tests carried out by EPA. The input data was transformed in such a way that they can be entered into the simulator. As a result of the simulator’s work, the instantaneous values of the key simulation parameters were obtained, which are presented in the figures below (Figure 6) [122].

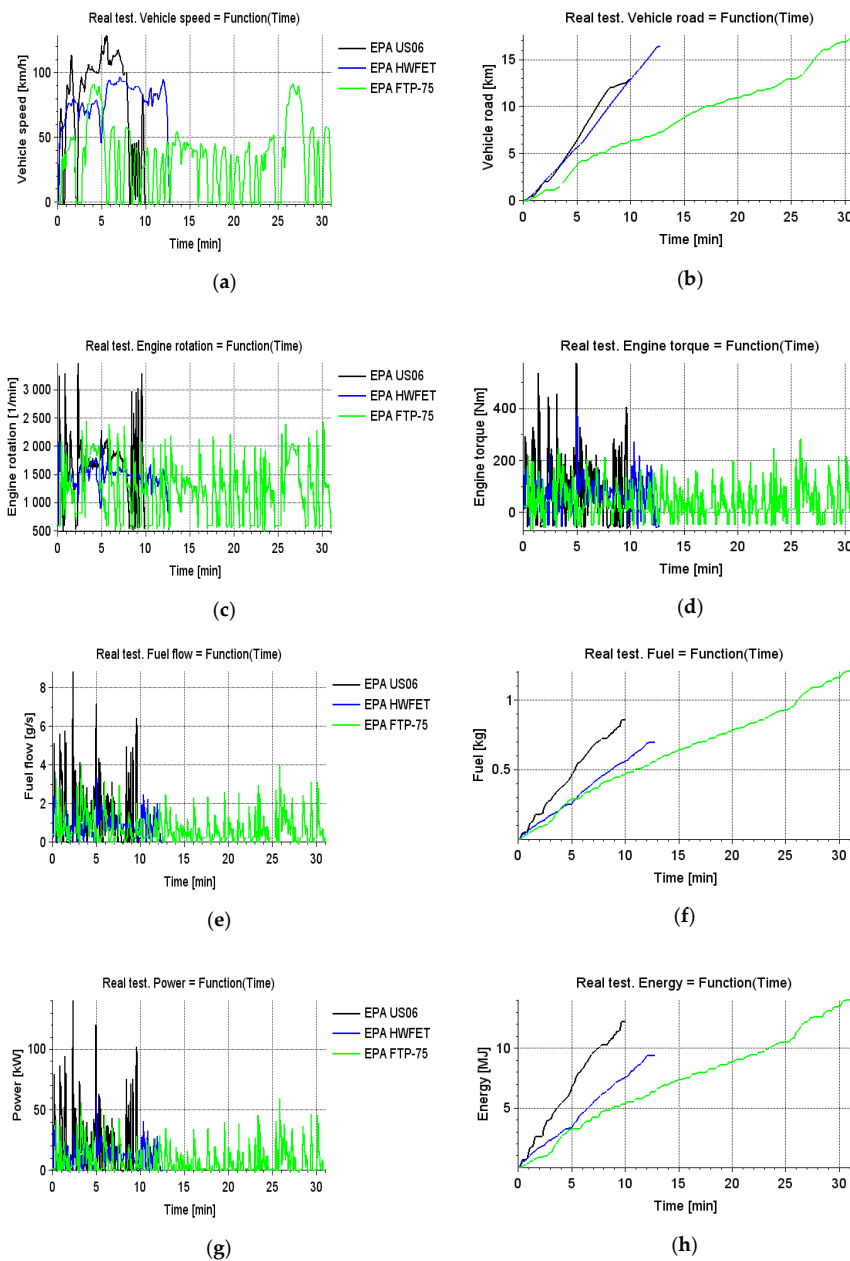


Figure 6. The results of the simulation work for the processed data from EPA tests for the 2013 Mercedes E350 vehicle: (a) Waveforms of the instantaneous vehicle speed values; (b) Waveforms of the instantaneous values of the distance travelled by the vehicle; (c) Waveforms of the instantaneous vehicle engine speed values; (d) Waveforms of the instantaneous values of torque generated by the vehicle engine; (e) Waveforms of the instantaneous values of the fuel stream powering the vehicle engine; (f) Waveforms of the instantaneous fuel consumption values for the vehicle; (g) Waveforms of the instantaneous values of power generated by the vehicle’s engine; (h) Waveforms of the instantaneous values of mechanical energy generated by the vehicle engine.

3.2. Simulation Work Results for the Introduced Driving Tests

On the basis of the prepared input data, using the “Gearshift Calculation Tool” programme, simulations were carried out of selected driving tests for the vehicle in question. Figure 7 below shows the waveforms of the instantaneous vehicle speed values in the test. These waveforms indicate large variability of this parameter in simulated tests, including the mean values, the dynamics of changes and the distribution of the values over time. The simulated tests were also characterized by high variability of the time of execution.

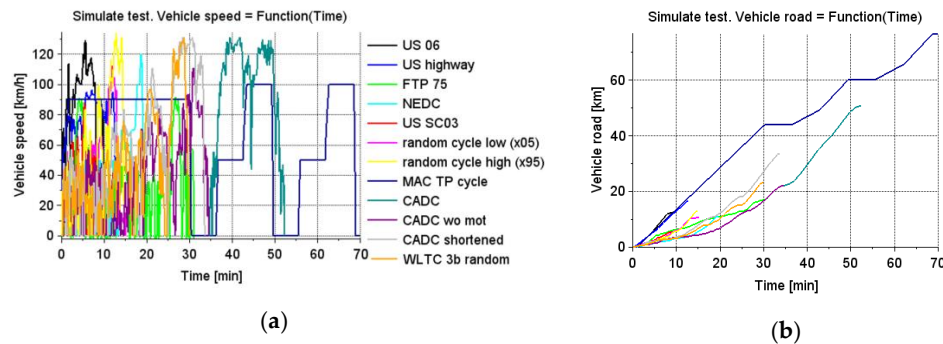


Figure 7. Results obtained in the simulation of selected road tests for the 2013 Mercedes E350 vehicle: (a) Waveforms of the instantaneous vehicle speed values; (b) Waveforms of the instantaneous values of the distance travelled by the vehicle.

Figure 8 below shows the waveforms of the instantaneous values of the travelled distance in the tests considered in the simulation.

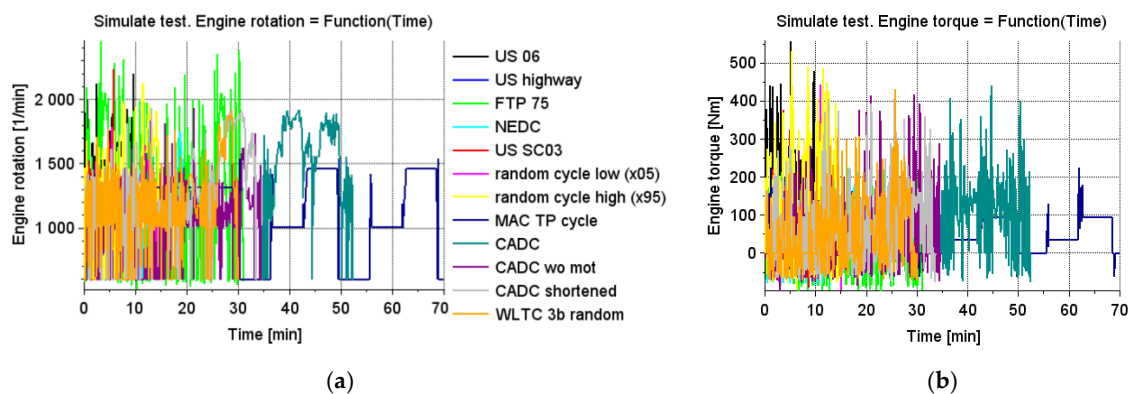


Figure 8. Results obtained in the simulation of selected road tests for the 2013 Mercedes E350 vehicle: (a) Waveforms of the instantaneous values of the vehicle engine rotational speed; (b) Waveforms of the instantaneous values of the torque generated by the vehicle engine.

Other input parameters for the driving test simulator were the instantaneous values of the engine rotational speed and the torque generated by the engine, whose waveforms are presented below.

In the developed driving test simulator, the instantaneous values of the power generated by the engine and the mechanical energy consumed during the test were calculated. Figure 9 shows the waveforms of these parameters.

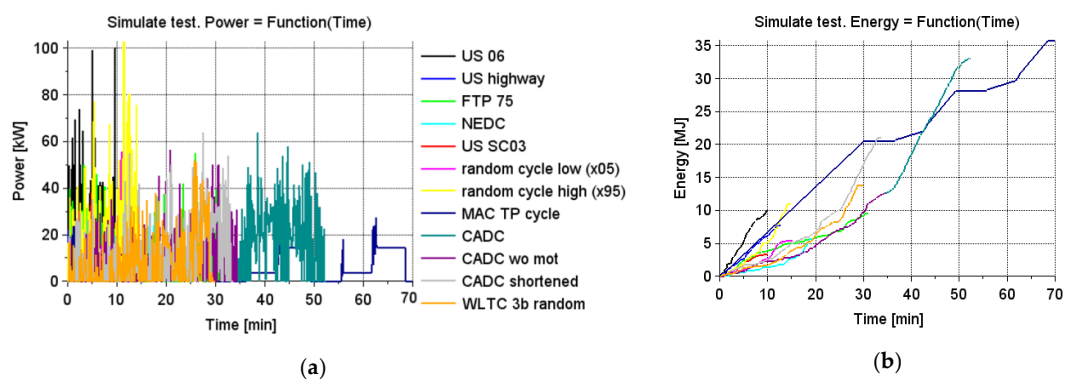


Figure 9. Results obtained in the simulation of selected road tests for the 2013 Mercedes E350 vehicle: (a) Waveforms of the instantaneous values of power generated by the engine; (b) Waveforms of the instantaneous values of mechanical energy generated by the vehicle engine.

3.3. Simulation Results for the Stream and Final Fuel Consumption for Selected Driving Tests and Fuels

On the basis of the diesel oil stream values calculated in the simulator, including the calorific values of the fuels in question, the instantaneous values of these fuels' streams and their mass consumption were calculated for the tests in question. The figures below summarize the obtained waveforms of the instantaneous values of fuel streams and the mass consumption of fuels in a given driving test in question (Figure 10).

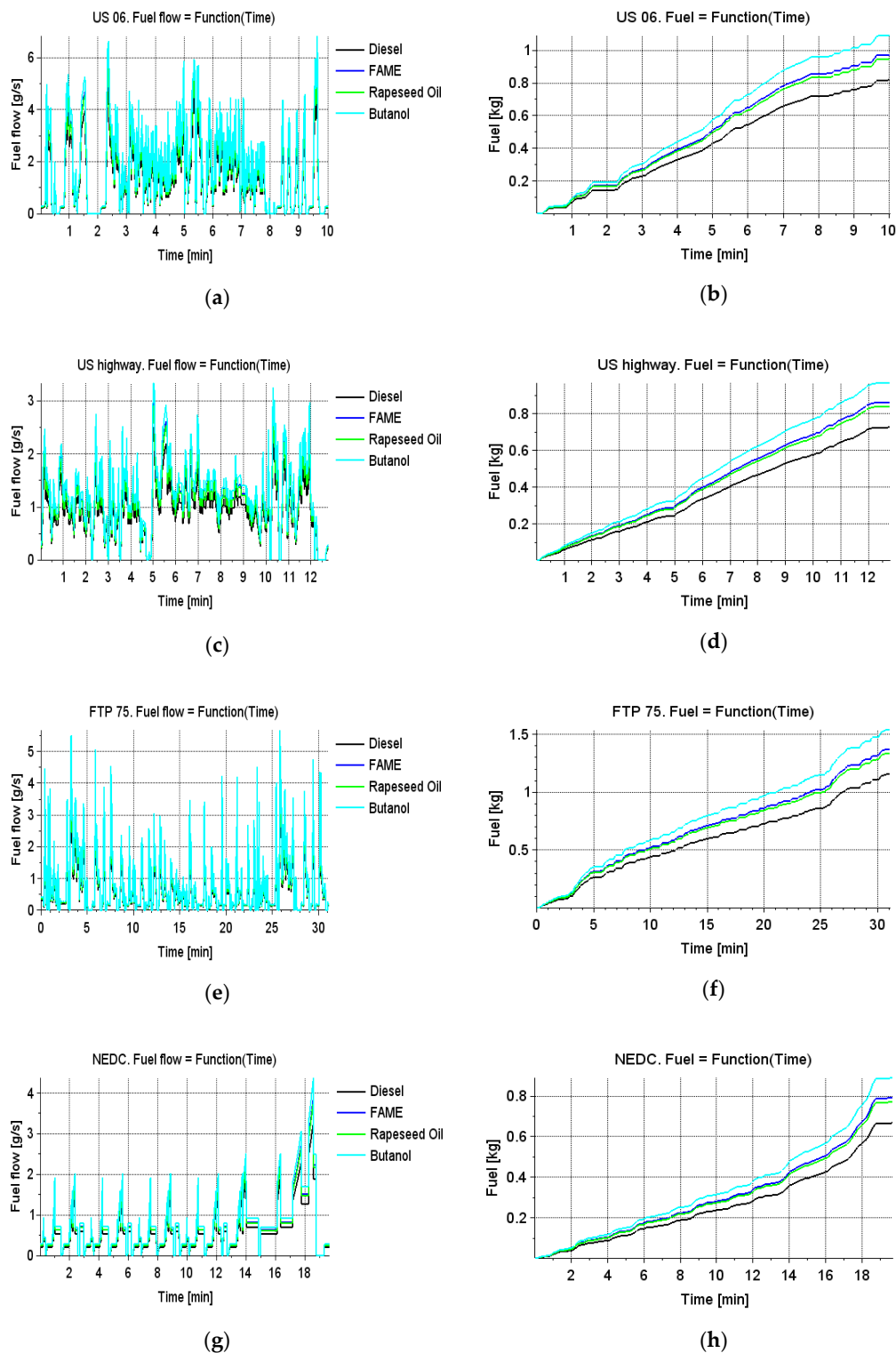


Figure 10. Cont.

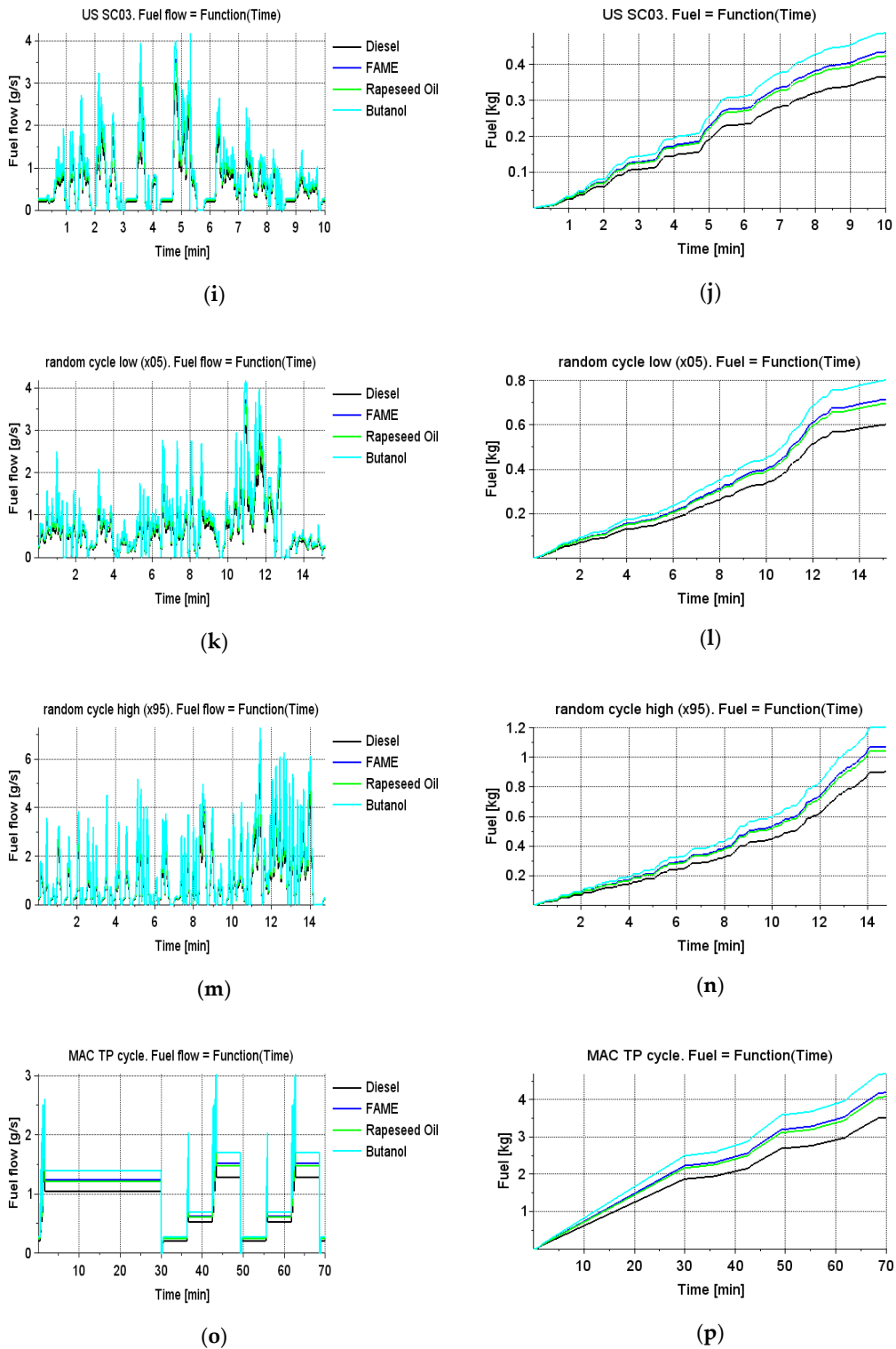


Figure 10. Cont.

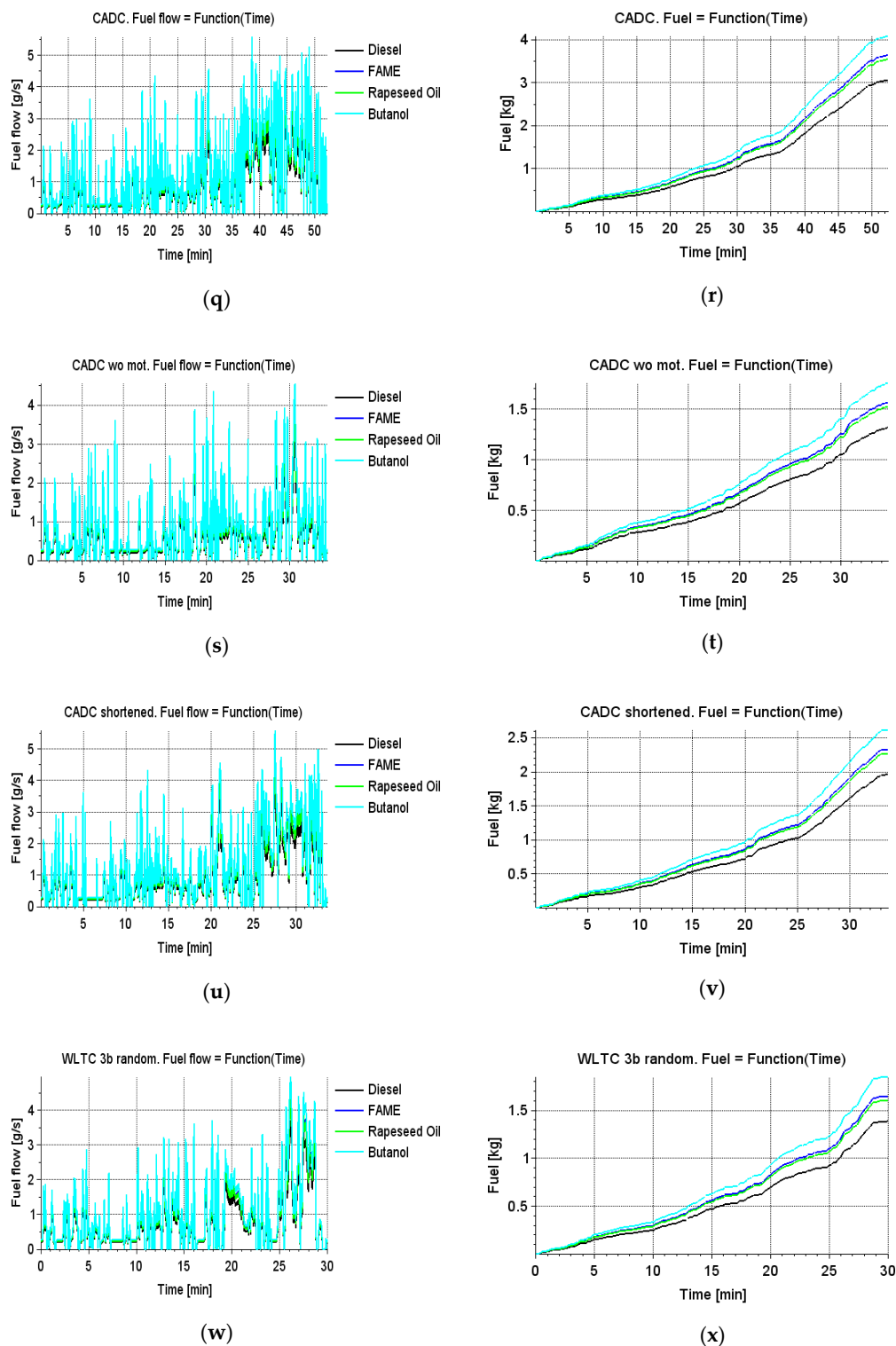


Figure 10. Results of the simulation of the stream and final fuel consumption for selected driving tests and selected fuels for the 2013 Mercedes E350 vehicle: (a) Waveforms of the instantaneous values of the fuel stream powering the vehicle's engine, obtained in the simulation of the US 06 road test; (b) Waveforms of the instantaneous values of fuel consumption for the vehicle, obtained in the simulation of the US 06 road test; (c) Waveforms of the instantaneous values of the fuel stream powering the vehicle's engine, obtained in the simulation of the US highway road test; (d) Waveforms of the instantaneous values fuel consumption values for the vehicle, obtained in the US highway test simulation; (e) Waveforms of the instantaneous values of the fuel stream powering the vehicle's engine, obtained in the simulation of the FTP 75 road test; (f) Waveforms of the instantaneous values of fuel consumption for the vehicle, obtained in the simulation of the FTP 75 road

test; (g) Waveforms of the instantaneous values of the fuel stream powering the vehicle's engine, obtained in the simulation of the NEDC road test; (h) Waveforms of the instantaneous values of fuel consumption for the vehicle, obtained in the simulation of the NEDC road test; (i) Waveforms of the instantaneous values of the fuel stream powering the vehicle's engine, obtained in the simulation of the US SC03 road test; (j) Waveforms of the instantaneous values of fuel consumption for the vehicle, obtained in the simulation of the US SC03 road test; (k) Waveforms of the instantaneous values of the fuel stream powering the vehicle's engine, obtained in the simulation of the Random Cycle Low (x05) road test; (l) Waveforms of the instantaneous values of fuel consumption for the vehicle, obtained in the simulation of the Random Cycle Low (x05) road test; (m) Waveforms of the instantaneous values of the fuel stream powering the vehicle's engine, obtained in the simulation of the Random Cycle High (x95) road test; (n) Waveforms of the instantaneous values of the fuel consumption for the vehicle, obtained in the simulation of the Random Cycle High (x95) road test; (o) Waveforms of the instantaneous values of the fuel stream powering the vehicle's engine, obtained in the simulation of the MAC TP cycle road test; (p) Waveforms of the instantaneous values of fuel consumption for the vehicle, obtained in the simulation of the MAC TP cycle road test; (q) Waveforms of the instantaneous values of the fuel stream powering the vehicle's engine, obtained in the simulation of the CADC road test; (r) Waveforms of the instantaneous values of fuel consumption for the vehicle, obtained in the simulation of the CADC road test; (s) Waveforms of the instantaneous values of the fuel stream powering the vehicle's engine, obtained in the simulation of the CADC without MOT road test; (t) Waveforms of the instantaneous values of fuel consumption for the vehicle, obtained in the simulation of the CADC without MOT road test; (u) Waveforms of the instantaneous values of the fuel stream powering the vehicle's engine, obtained in the simulation of the CADC shortened road test; (v) Waveforms of the instantaneous values of fuel consumption for the vehicle, obtained in the simulation of the CADC shortened road test; (w) Waveforms of the instantaneous values of the fuel stream powering the vehicle's engine, obtained in the simulation of the WLTC 3b random road test; (x) Waveforms of the instantaneous values of fuel consumption for the vehicle, obtained in the simulation of the WLTC 3b random road test.

3.4. The Results of the Simulation of Carbon Dioxide Flux and Emission for Selected Driving Tests and Fuels

As a result of the vehicle simulation processes carried out for selected driving tests, taking into account various fuels, the instantaneous values of the carbon dioxide flux and its emissivity during the test were obtained. The figures below (Figure 11) show the results of the simulator's work in the form of carbon dioxide streams and its emissivity, taking into account the fuels considered for individual simulated tests.

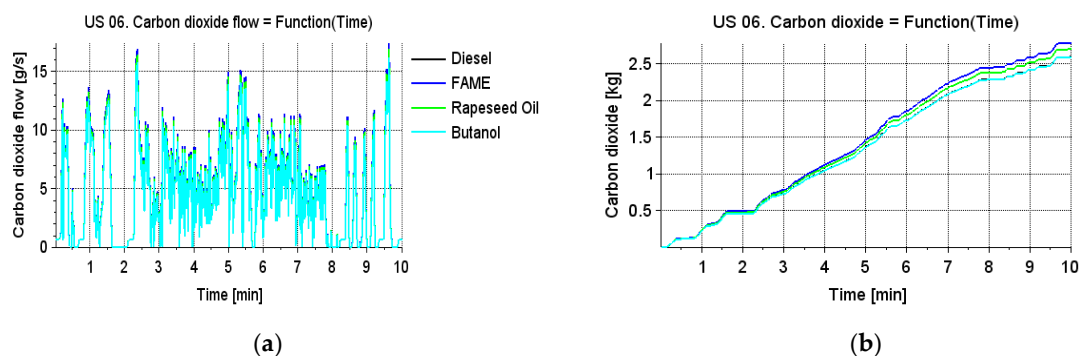


Figure 11. Cont.

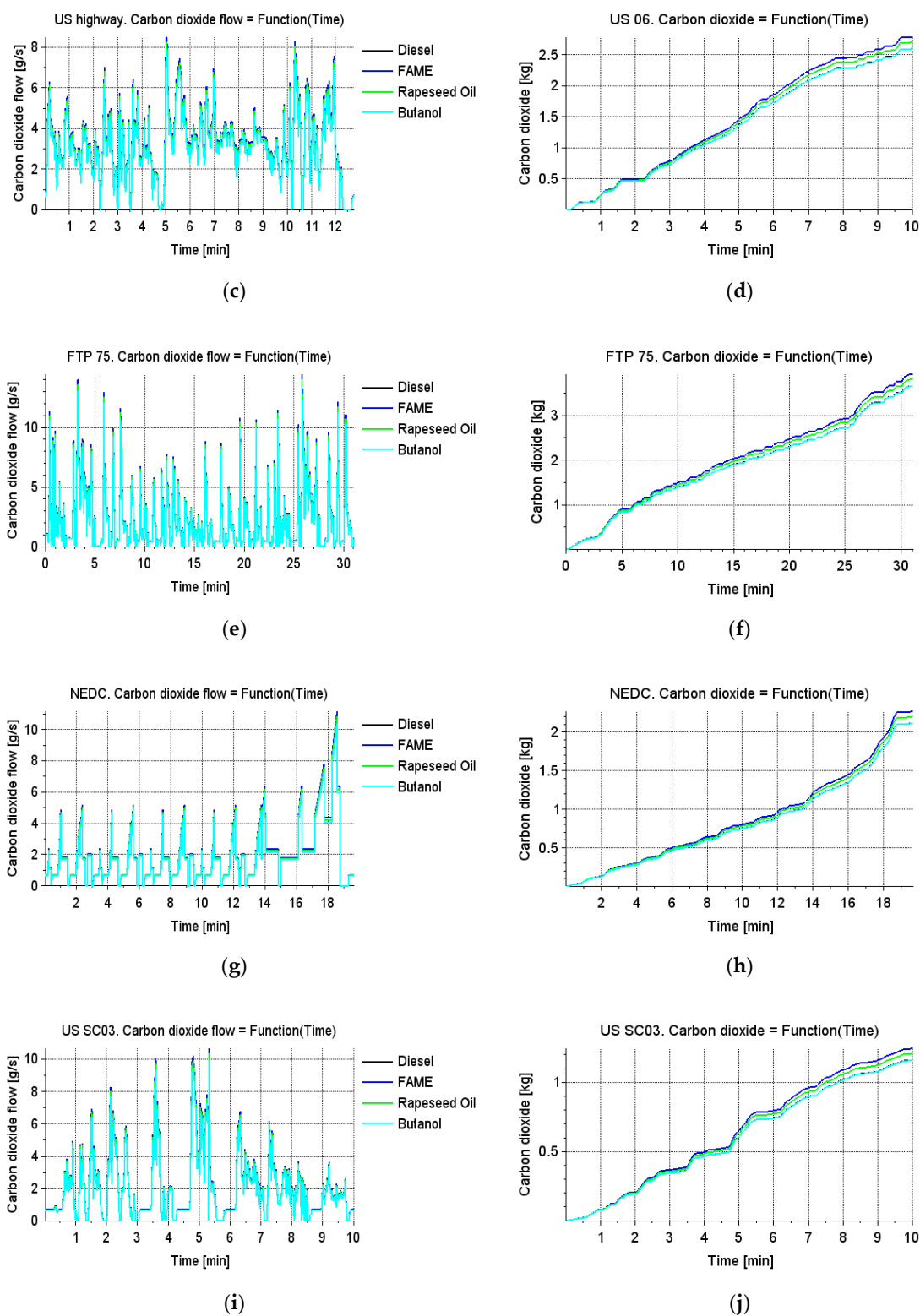


Figure 11. Cont.

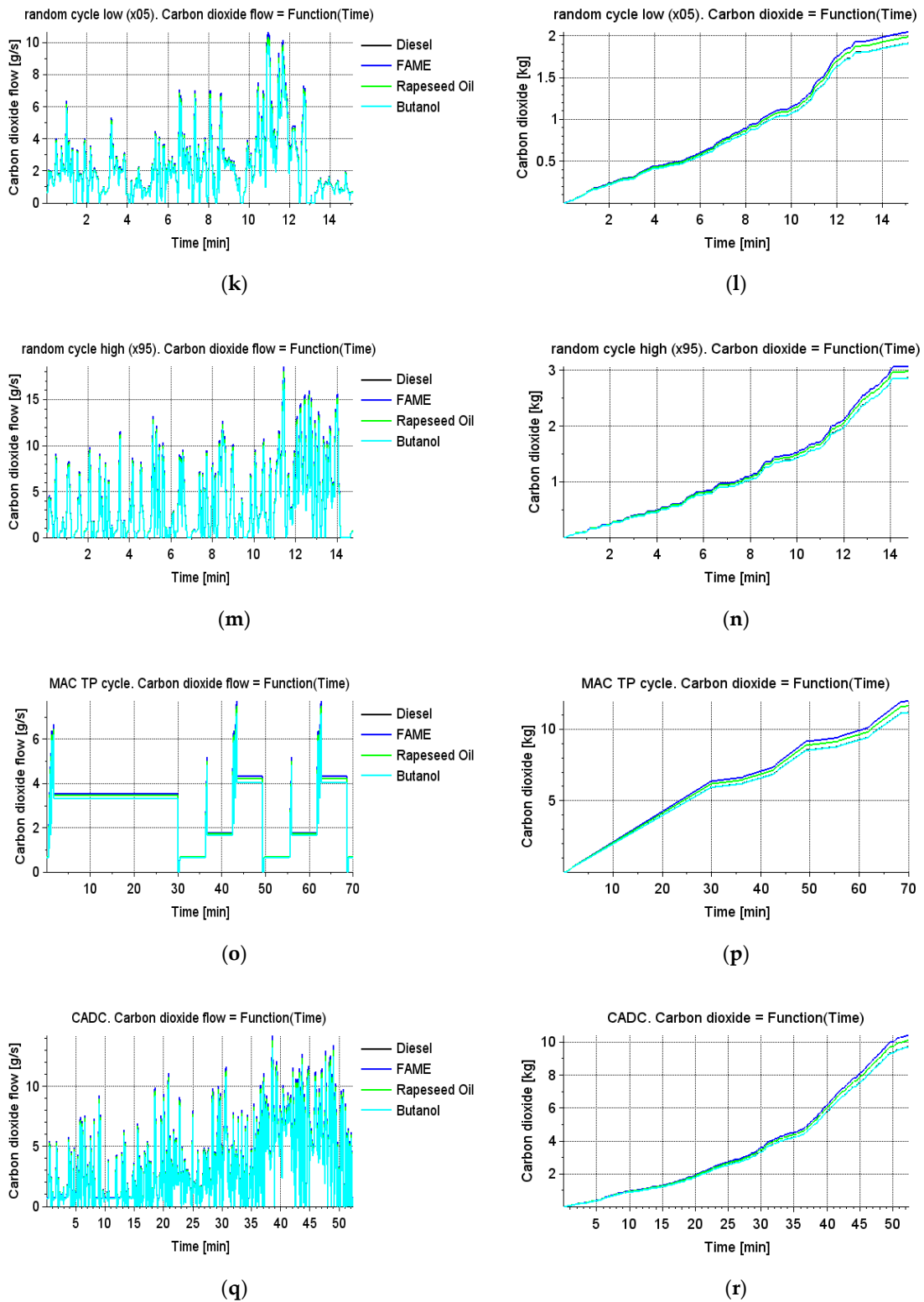


Figure 11. Cont.

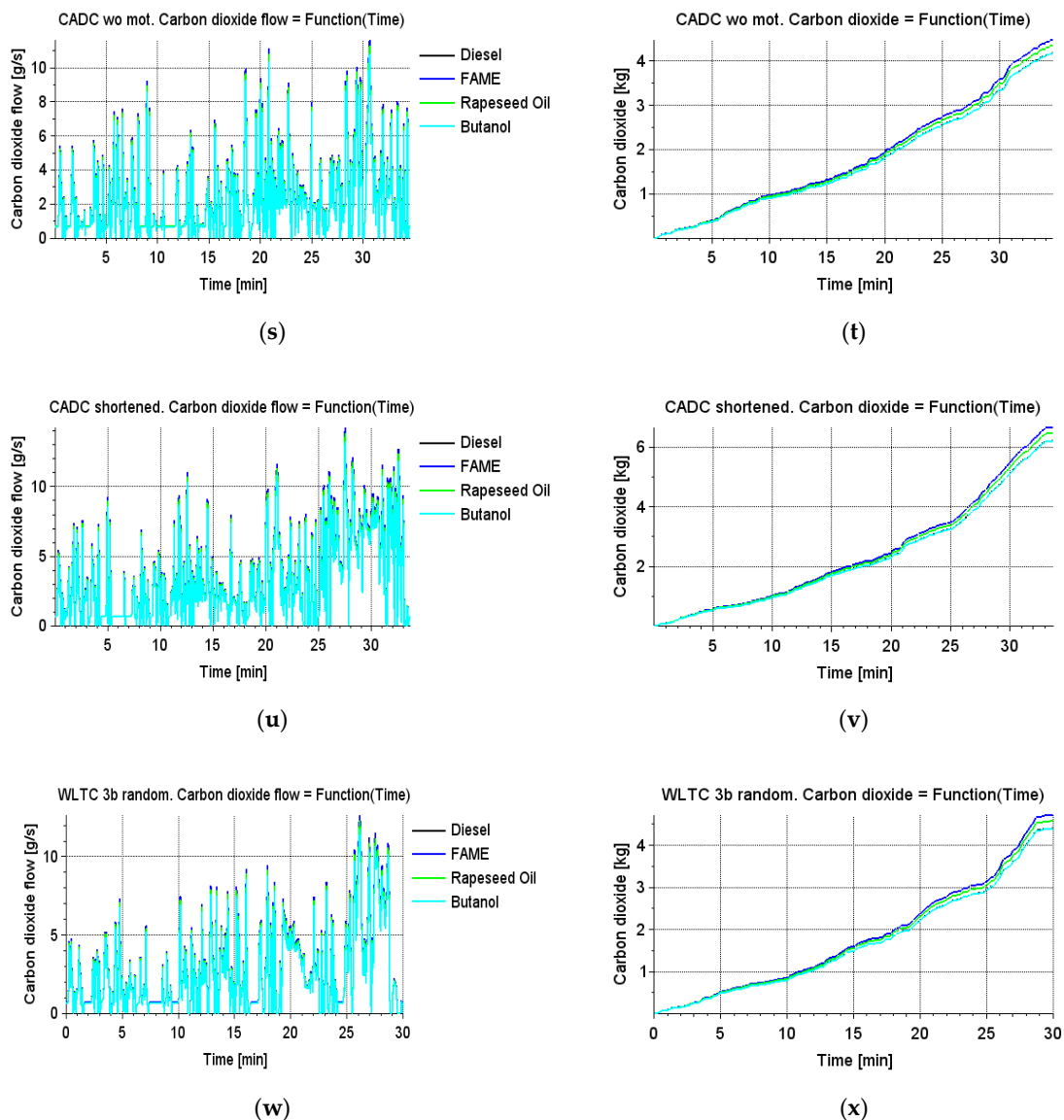


Figure 11. The results of the simulation of the carbon dioxide stream and emission for selected driving tests and fuels for the 2013 Mercedes E350 vehicle: (a) Waveforms of the instantaneous values of the carbon dioxide emission stream produced by the vehicle engine, obtained in the simulation of the US 06 road test; (b) Waveforms of the instantaneous values of the carbon dioxide emission produced by the vehicle engine, obtained in the simulation of the US 06 road test; (c) Waveforms of the instantaneous values of the carbon dioxide emission stream produced by the vehicle engine, obtained in the simulation of the US Highway road test; (d) Waveforms of the instantaneous values of the carbon dioxide emission produced by the vehicle engine, obtained in the simulation of the US Highway road test; (e) Waveforms of the instantaneous values of the carbon dioxide emission stream produced by the vehicle engine, obtained in the simulation of the FTP 75 road test; (f) Waveforms of the instantaneous values of the carbon dioxide emission produced by the vehicle engine, obtained in the simulation of the FTP 75 road test; (g) Waveforms of the instantaneous values of the carbon dioxide emission stream produced by the vehicle engine, obtained in the simulation of the NEDC road test; (h) Waveforms of the instantaneous values of the carbon dioxide emission produced by the vehicle engine, obtained in the simulation of the US 06 road test; (i) Waveforms of the instantaneous values of the carbon dioxide emission stream produced by the vehicle engine, obtained in the simulation of the US SC03 road test; (j) Waveforms of the instantaneous values of the carbon dioxide emission produced by the vehicle engine, obtained in the simulation of the US SC03 road test; (k) Waveforms of the instantaneous values of the carbon dioxide emission stream produced by the vehicle engine, obtained in the simulation of the Random Cycle Low road test (x05); (l) Waveforms of the instantaneous values of the carbon dioxide emission produced by the vehicle engine, obtained in the simulation of the Random Cycle Low road test (x05); (m) Waveforms of the instantaneous values of the carbon dioxide

emission stream produced by the vehicle engine, obtained in the simulation of the Random Cycle High road test (x95); (n) Waveforms of the instantaneous values of the carbon dioxide emission produced by the vehicle engine, obtained in the simulation of the Random Cycle High (x95) road test; (o) Waveforms of the instantaneous values of the carbon dioxide emission stream produced by the vehicle engine, obtained in the simulation of the MAC TP road test; (p) Waveforms of the instantaneous values of the carbon dioxide emission produced by the vehicle engine, obtained in the simulation of the MAC TP road test; (q) Waveforms of the instantaneous values of the carbon dioxide emission stream produced by the vehicle engine, obtained in the simulation of the CADC road test; (r) Waveforms of the instantaneous values of the carbon dioxide emission produced by the vehicle engine, obtained in the simulation of the CADC road test; (s) Waveforms of the instantaneous values of the carbon dioxide emission stream produced by the vehicle engine, obtained in the simulation of the CADC without MOT road test; (t) Waveforms of the instantaneous values of the carbon dioxide emission produced by the vehicle engine, obtained in the simulation of the CADC without MOT road test; (u) Waveforms of the instantaneous values of the carbon dioxide emission stream produced by the vehicle engine, obtained in the simulation of the CADC shortened road test; (v) Waveforms of the instantaneous values of the carbon dioxide emission produced by the vehicle engine, obtained in the simulation of the CADC shortened road test; (w) Waveforms of the instantaneous values of the carbon dioxide emission stream produced by the vehicle engine, obtained in the simulation of the WLTC 3b random road test; (x) Waveforms of the instantaneous values of the carbon dioxide emission produced by the vehicle engine, obtained in the simulation of the WLTC 3b road test.

4. Discussion

A computer simulation is an economical and time-effective alternative to replace costly road tests. It is especially important in the early stages of the product line development cycle. The driving cycle is only an approximation of the vehicle operating conditions on the road. It is performed on a chassis dynamometer. The vehicle is immobilized throughout the test. By applying a load by means of rollers, usually connected to electrical machines, the axles of the vehicle are driven. Road loads (aerodynamics, inertia) must be simulated by a dynamometer.

The developed computer tool is used to analyze fuel consumption and CO₂ emissions in the context of driving tests and the fuels used.

Figure 12 presents the results of the simulator work for the fuels in question and driving tests in the form of the fuel consumption parameter per one kilometer travelled in the test. For diesel, the minimum value was reached at the level of 44 g/km for the US highway driving test, while the maximum value was obtained at the Random Cycle High (x95) test (69.8 g/km). In the case of the biofuels in question, this parameter indicates an increase in the biofuel demand in the simulated tests in relation to diesel fuel. For these biofuels, the increase in relation to diesel fuel approximately amounted to: rapeseed oil—16%, FAME—19%, butanol—33%. The main reason for the increase in the engine's demand for biofuels is their much lower calorific value in relation to diesel oil.

Figure 13 presents the results of the simulator work for the fuels and driving tests in question, in the form of the carbon dioxide emission parameter per one kilometer travelled in the test. For diesel, the minimum value was achieved at the level of 140 g/km for the US highway test, while the maximum value was obtained at the Random Cycle High (x95) test (221 g/km). In the case of the biofuels in question, the changes in the values of carbon dioxide emissions per one kilometer of the distance travelled in relation to diesel oil were approximately: rapeseed oil—4%, FAME—7.2%, butanol—0.2%. The main reason for the changes in the carbon dioxide emissivity of these fuels in relation to diesel oil is their chemical composition.

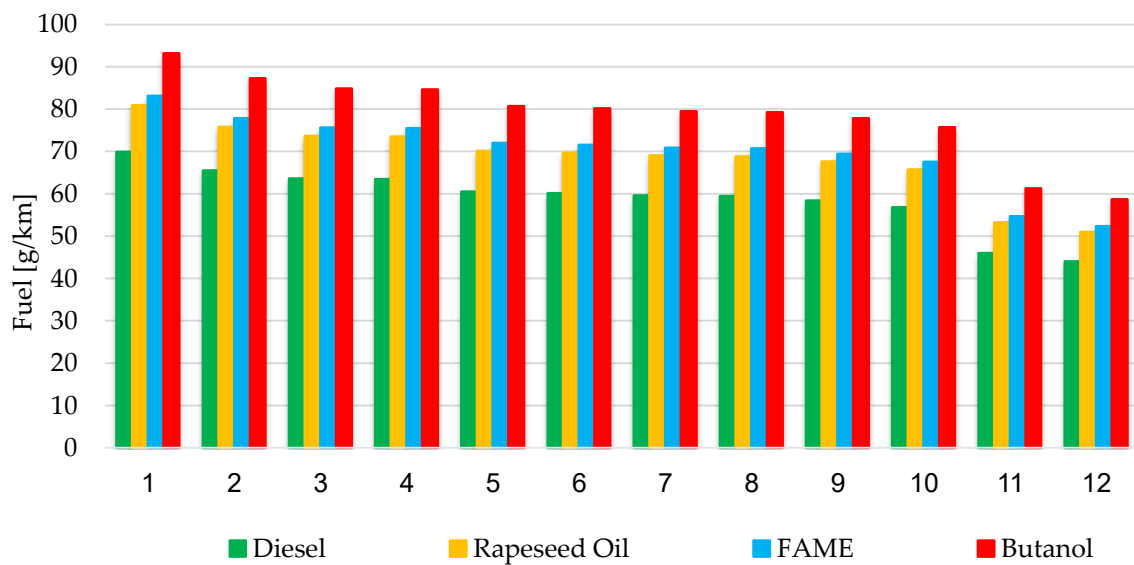


Figure 12. Summary of fuel mass consumption in tests per 1 kilometer: 1—Random Cycle High (x95); 2—FTP 75; 3—US SC03; 4—US 06; 5—NEDC; 6—CADC; 7—WLTC 3b random; 8—CADC without MOT; 9—CADC shortened; 10—Random Cycle Low (x05); 11—MAC TP cycle; 12—US highway.

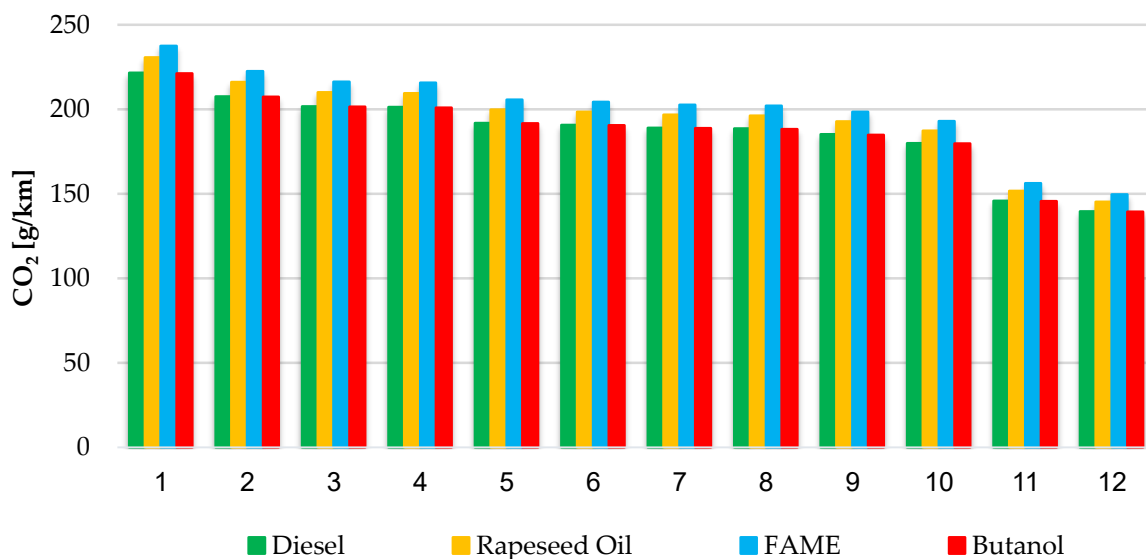


Figure 13. Summary of carbon dioxide emissions in tests per 1 kilometer: 1—Random Cycle High (x95); 2—FTP 75; 3—US SC03; 4—US 06; 5—NEDC; 6—CADC; 7—WLTC 3b random; 8—CADC without MOT; 9—CADC shortened; 10—Random Cycle Low (x05); 11—MAC TP cycle; 12—US highway.

Figure 14 shows the data obtained from the simulations of driving tests, including biofuels, in the form of the mass consumption parameter of a given fuel per unit of mechanical energy produced (1 kilowatt hour). For diesel, the minimum value was achieved at the level of 297 g/kWh for the Random Cycle High (x95) driving test, while the maximum value was obtained for the FTP 75 test (434 g/kWh). In the case of the biofuels in question, the changes in the values of carbon dioxide emissions per one kilometer of the distance travelled in relation to diesel fuel approximately amounted to: rapeseed oil—16%, FAME—19%, butanol—33%.

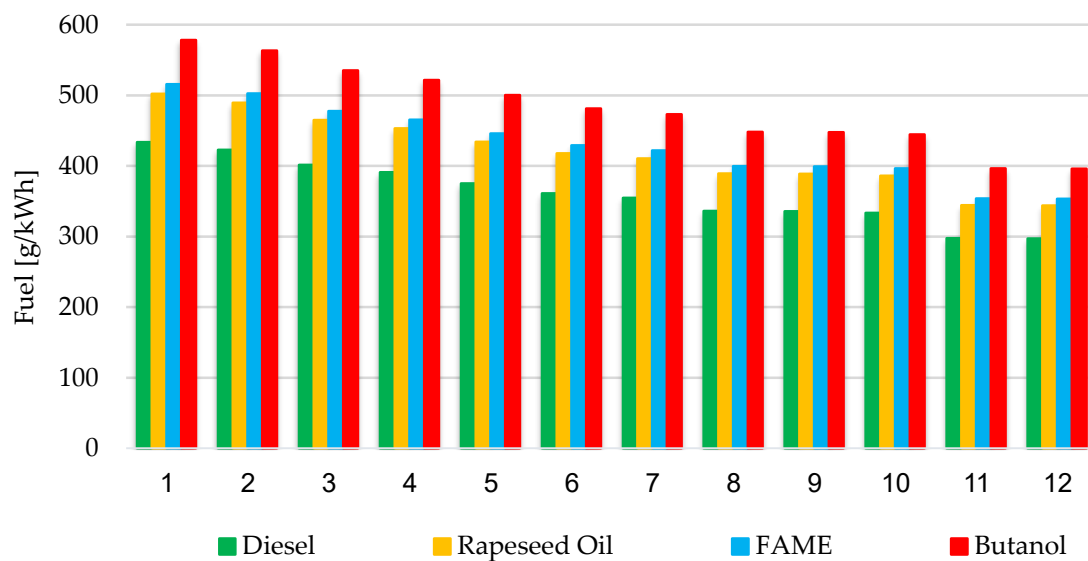


Figure 14. Summary of fuel mass consumption in tests per 1 kilowatt hour: 1—FTP 75; 2—NEDC; 3—Random Cycle Low (x05); 4—US SC03; 5—CADC without MOT; 6—WLTC 3b random; 7—MAC TP cycle; 8—US highway; 9—CADC shortened; 10—CADC; 11—US 06; 12—Random Cycle High (x95).

Figure 15 presents the results of the simulator work for the considered fuels and driving tests in the form of the carbon dioxide emission parameter per unit of mechanical energy produced (1 kilowatt hour). For diesel, the minimum value was achieved at 942 g/kWh for the Random Cycle High (x95) driving test, while the maximum value was obtained for the FTP 75 (x95) test (g/kWh). In the case of the biofuels in question, the changes in the values of carbon dioxide emissions per one kilometer of the distance travelled in relation to diesel oil were approximately: rapeseed oil—4%, FAME—7.2%, butanol—0.2%.

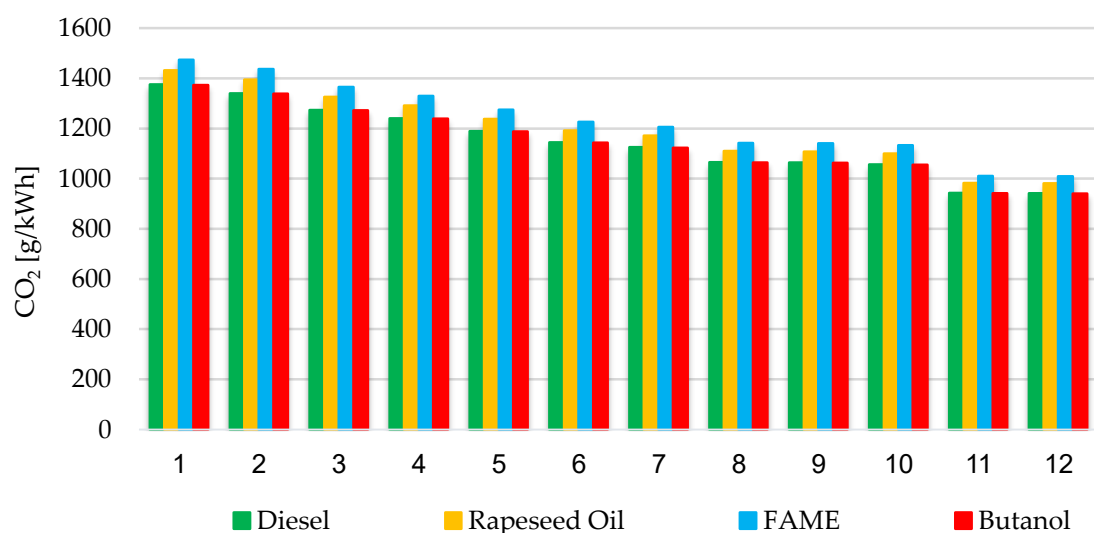


Figure 15. Summary of carbon dioxide emissions in tests for 1 kilowatt hour: 1—FTP 75; 2—NEDC; 3—Random Cycle Low (x05); 4—US SC03; 5—CADC without MOT; 6—WLTC 3b random; 7—MAC TP cycle; 8—US highway; 9—CADC shortened; 10—CADC; 11—US 06; 12—Random Cycle High (x95).

5. Conclusions

The paper presents a computer tool for simulating driving tests valid in the European Union and outside it (e.g., in the USA), developed in the Scilab 6.1.0 program. The

developed simulator uses the data created with the use of the “Gearshift Calculation Tool” programme, the results from the process of optimization of the neural network structures and the properties of the biofuels in question.

- There were 12 drive tests analyzed in this study. These tests differed from one another in terms of the distance required to be covered by the car during the test and the speed achieved. An additional parameter was the inclusion of the additional fuel consumption and pollutant emissions caused by the operation of the mobile air conditioning system.
- The neural model used in the developed computer tool made it possible to calculate the instantaneous value of the fuel stream as a function of the engine rotational speed, the torque generated by the engine, the gear number in the transmission and the vehicle speed. The data obtained during the 2013 Mercedes E350 vehicle tests on a chassis dynamometer were used for its construction.
- Multilayer Feedforward Backpropagation Neural Networks with approximating properties were used to build the neural model. The Levenberg–Marquardt algorithm was used in the network learning process. The relative error for the selected neural network structure was 4.7%.
- Taking into account the consumption of a given fuel per kilometer in the test for diesel fuel, the minimum value was achieved at the level of 44 g/km for the US Highway driving test. The diesel maximum value was achieved in the Random Cycle High (x95) driving test (69.8 g/km). In the case of the biofuels used, the demand was higher in relation to diesel oil: rapeseed oil—16%, FAME—19%, butanol—33%. This was due to the generally lower calorific value of biofuels.
- When analyzing the emission of carbon dioxide per kilometer for diesel fuel, the minimum value was achieved at 140 g/km for the US Highway driving test, while the maximum value was achieved in the Random Cycle High (x95) test (221 g/km). In the case of the analyzed biofuels, the emission of carbon dioxide per one kilometer of the distance travelled in relation to diesel fuel was as follows: rapeseed oil—4%, FAME—7.2%, butanol—0.2%.
- From the point of view of the parameter of the mass consumption of fuel per unit of mechanical energy generated (1 kilowatt hour) for diesel fuel, the minimum value achieved in the simulation test was 297 g/kWh for the Random Cycle High drive test (x95), while the maximum value was obtained for the FTP 75 test (434 g/kWh).
- However, when analyzing the emission of carbon dioxide per unit of mechanical energy generated (1 kilowatt hour) for diesel, the minimum value was 942 g/kWh for the Random Cycle High driving test (x95) and the maximum value was obtained for the FTP 75 (x95) test (g/kWh). The changes in the values of carbon dioxide emissions per one kilometer of the distance travelled in relation to diesel fuel were as follows: rapeseed oil—4%, FAME—7.2%, butanol—0.2%.

The aim of the research was to obtain information, generated by a constructed computer tool using neural networks to simulate driving tests, about CO₂ emissions when using different fuels. Therefore, in the manuscript, the author focused on building a solution which is a computer simulation that would allow to estimate the instantaneous consumption of the various fuels used so as to provide an equal amount of chemical energy contained in the fuels at later stages, in which part of this energy is converted into work. Taking into account the chemical composition of the fuel (including the share of carbon, hydrogen, oxygen) and according to the chemical reactions of the fuel combustion processes, the momentary values of the CO₂ stream are calculated.

The manuscript uses the test results of the Mercedes E350 published by the EPA as a basis for building a computer simulation. Analyses of the work of the developed ALPHA EPA solution made it possible to put forward a hypothesis that it is possible to obtain a quantitative model of specific fuel consumption as a function of engine speed, torque generated by the engine, transmission ratio using neural networks with a reverse error propagation algorithm Levenberg–Marquardt learning algorithm characterized by a high

degree of matching to research data. The proposed solution will enable in future research work to develop simplified models for many vehicles and to build large structures to simulate the emissivity and fuel consumption of many vehicles in urban and extra-urban driving conditions, which could affect critical areas of roads with high traffic intensity and its impact on the environment. Learning processes of many neural network structures were carried out, resulting in satisfactory accuracy of quantitative models, comparable to other research projects.

The developed neural model is only a part of the simulation, the results of which are presented in the manuscript. The simulation also has elements that allow for engine calculations based on vehicle dynamics, calculations based on loads corresponding to rolling losses and aerodynamic loads of a moving vehicle in accordance with the assumptions made by the EPA in real driving tests.

Funding: The APC was funded by Institute of Mechanical Engineering, Warsaw University of Life Sciences.

Institutional Review Board Statement: Not applicable.

Informed Consent Statement: Not applicable.

Data Availability Statement: All data are presented in this article. Data sharing is not applicable to this article.

Conflicts of Interest: The author declare no conflict of interest.

References

- Zhao, X.; Ke, Y.; Zuo, J.; Xiong, W.; Wu, P. Evaluation of sustainable transport research in 2000–2019. *J. Clean. Prod.* **2020**, *256*, 120404. [[CrossRef](#)]
- Tian, N.; Tang, S.; Che, A.; Wu, P. Measuring regional transport sustainability using super-efficiency SBM-DEA with weighting preference. *J. Clean. Prod.* **2020**, *242*, 118474. [[CrossRef](#)]
- Nieuwenhuijsen, M.J. Urban and transport planning pathways to carbon neutral, liveable and healthy cities; A review of the current evidence. *Environ. Int.* **2020**, *140*, 105661. [[CrossRef](#)]
- Govender, P.; Sivakumar, V. Application of k-means and hierarchical clustering techniques for analysis of air pollution: A review (1980–2019). *Atmos. Pollut. Res.* **2020**, *11*, 40–56. [[CrossRef](#)]
- Takahashi, M.; Feng, Z.; Mikhailova, T.A.; Kalugina, O.V.; Shergina, O.V.; Afanasieva, L.V.; Heng, R.K.J.; Majid, N.M.A.; Sase, H. Air pollution monitoring and tree and forest decline in East Asia: A review. *Sci. Total Environ.* **2020**, *742*, 140288. [[CrossRef](#)]
- Tilt, B. China's air pollution crisis: Science and policy perspectives. *Environ. Sci. Policy* **2019**, *92*, 275–280. [[CrossRef](#)]
- Dey, S.; Dhal, G.C. Controlling carbon monoxide emissions from automobile vehicle exhaust using copper oxide catalysts in a catalytic converter. *Mater. Today Chem.* **2020**, *17*, 100282. [[CrossRef](#)]
- Reis, H.; Reis, C.; Sharip, A.; Reis, W.; Zhao, Y.; Sinclair, R.; Beeson, L. Diesel exhaust exposure, its multi-system effects, and the effect of new technology diesel exhaust. *Environ. Int.* **2018**, *114*, 252–265. [[CrossRef](#)]
- Puricelli, S.; Cardellini, G.; Casadei, S.; Faedo, D.; Van den Oever, A.E.M.; Grosso, M. A review on biofuels for Light-Duty vehicles in Europe. *Renew. Sustain. Energy Rev.* **2020**, *137*, 110398. [[CrossRef](#)]
- Leach, F.; Kalghatgi, G.; Stone, R.; Miles, P. The scope for improving the efficiency and environmental impact of internal combustion engines. *Transp. Eng.* **2020**, *1*, 100005. [[CrossRef](#)]
- Gohoungodji, P.; N'Dri, A.B.; Latulippe, J.M.; Matos, A.L.B. What is stopping the automotive industry from going green? A systematic review of barriers to green innovation in the automotive industry. *J. Clean. Prod.* **2020**, *277*, 123524. [[CrossRef](#)]
- Giampieri, A.; Ling-Chin, J.; Ma, Z.; Smallbone, A.; Roskilly, A.P. A review of the current automotive manufacturing practice from an energy perspective. *Appl. Energy* **2020**, *261*, 114074. [[CrossRef](#)]
- Shen, Z.G.; Tian, L.L.; Liu, X. Automotive exhaust thermoelectric generators: Current status, challenges and future prospects. *Energy Convers. Manag.* **2019**, *195*, 1138–1173. [[CrossRef](#)]
- Tucki, K.; Orynych, O.; Swi c, A.; Mitoraj-Wojtanek, M. The Development of Electromobility in Poland and EU States as a Tool for Management of CO₂ Emissions. *Energies* **2019**, *12*, 2942. [[CrossRef](#)]
- Kluschke, P.; Gnann, T.; Pl tz, P.; Wietschel, M. Market diffusion of alternative fuels and powertrains in heavy-duty vehicles: A literature review. *Energy Rep.* **2019**, *5*, 1010–1024. [[CrossRef](#)]
- The End of the Road? An Overview of Combustionengine Car Phase-Out Announcements across Europe. Available online: <https://theicct.org/sites/default/files/publications/Combustion-engine-phase-out-briefing-may11.2020.pdf> (accessed on 1 November 2020).
- Internal Combustion Engines (ICE) Counted for over 90% of Global Car Sales in H1 2019. Available online: <https://www.jato.com/internal-combustion-engines-ice-counted-for-over-90-of-global-car-sales-in-h1-2019/> (accessed on 1 November 2020).

18. Growing Momentum: Global Overview of Government Targets for Phasing out Sales of New Internal Combustion Engine Vehicles. Available online: <https://www.automotiveworld.com/news-releases/growing-momentum-global-overview-of-government-targets-for-phasing-out-sales-of-new-internal-combustion-engine-vehicles/> (accessed on 5 January 2021).
19. 2020 US Auto Sales by Model Analysis. Available online: <https://www.goodcarbadcar.net/2020-us-vehicle-sales-figures-by-model/> (accessed on 1 November 2020).
20. Deloitte. Future of Automotive Sales and Aftersales. Available online: <https://www2.deloitte.com/content/dam/Deloitte/global/Documents/Consumer-Business/gx-deloitte-future-of-automotive-sales-aftersales.pdf> (accessed on 1 November 2020).
21. Tucki, K.; Orynych, O.; Mitoraj-Wojtanek, M. Perspectives for Mitigation of CO₂ Emission due to Development of Electromobility in Several Countries. *Energies* **2020**, *13*, 4127. [[CrossRef](#)]
22. Fuel Types of New Passenger Cars. Available online: <https://www.acea.be/statistics/tag/category/share-of-diesel-in-new-passenger-cars> (accessed on 1 November 2020).
23. Hoofman, N.; Messagie, M.; Van Mierlo, J.; Coosemans, T. A review of the European passenger car regulations—Real driving emissions vs local air quality. *Renew. Sustain. Energy Rev.* **2018**, *86*, 1–21. [[CrossRef](#)]
24. Worldwide Emission Standards and Related Regulations. Passenger Cars/Light and Medium Duty Vehicles May 2019. Available online: https://www.continental-automotive.com/getattachment/8f2dedad-b510-4672-a005-3156f77d1f85/EMISSIONBOOKLET_2019.pdf (accessed on 1 November 2020).
25. Dou, X.; Linn, J. How do US passenger vehicle fuel economy standards affect new vehicle purchases? *J. Environ. Econ. Manag.* **2020**, *102*, 102332. [[CrossRef](#)]
26. Gao, J.; Chen, H.; Li, Y.; Chen, J.; Zhang, Y.; Dave, K.; Huang, Y. Fuel consumption and exhaust emissions of diesel vehicles in worldwide harmonized light vehicles test cycles and their sensitivities to eco-driving factors. *Energy Convers. Manag.* **2019**, *196*, 605–613. [[CrossRef](#)]
27. Ho, S.; Wong, Y.; Chang, V.W. Developing Singapore Driving Cycle for passenger cars to estimate fuel consumption and vehicular emissions. *Atmos. Environ.* **2014**, *97*, 353–362. [[CrossRef](#)]
28. Quirama, L.F.; Giraldo, M.; Huertas, J.I.; Jaller, M. Driving cycles that reproduce driving patterns, energy consumptions and tailpipe emissions. *Transp. Res. Part D Transp. Environ.* **2020**, *82*, 102294. [[CrossRef](#)]
29. Cha, J.; Lee, J.; Chon, M.S. Evaluation of real driving emissions for Euro 6 Light-Duty diesel vehicles equipped with LNT and SCR on domestic sales in Korea. *Atmos. Environ.* **2019**, *196*, 133–142. [[CrossRef](#)]
30. Wihersaari, H.; Pirjola, L.; Karjalainen, P.; Saukko, E.; Kuuluvainen, H.; Kulmala, K.; Keskinen, J.; Rönkkö, T. Particulate emissions of a modern diesel passenger car under laboratory and real-world transient driving conditions. *Environ. Pollut.* **2020**, *265*, 114948. [[CrossRef](#)] [[PubMed](#)]
31. Pisani, E.; Andriollo, E.; Masiero, M.; Secco, L. Intermediary organisations in collaborative environmental governance: Evidence of the EU-funded LIFE sub-programme for the environment (LIFE-ENV). *Heliyon* **2020**, *6*, e04251. [[CrossRef](#)] [[PubMed](#)]
32. Kiba-Janiak, M. EU cities' potentials for formulation and implementation of sustainable urban freight transport strategic plans. *Transp. Res. Procedia* **2019**, *39*, 150–159. [[CrossRef](#)]
33. García-Álvarez, M.T.; Moreno, B. Environmental performance assessment in the EU: A challenge for the sustainability. *J. Clean. Prod.* **2018**, *205*, 266–280. [[CrossRef](#)]
34. Neves, S.A.; Marques, A.C.; Patrício, M. Determinants of CO₂ emissions in European Union countries: Does environmental regulation reduce environmental pollution? *Econ. Anal. Policy* **2020**, *68*, 114–125. [[CrossRef](#)]
35. Rubio, F.; Llopis-Albert, C.; Valero, F.; Besa, A.J. Sustainability and optimization in the automotive sector for adaptation to government vehicle pollutant emission regulations. *J. Bus. Res.* **2020**, *112*, 561–566. [[CrossRef](#)]
36. Krause, J.; Thiel, C.; Tsokolis, D.; Samaras, Z.; Rota, C.; Ward, A.; Prenninger, P.; Coosemans, T.; Neugebauer, S.; Verhoeve, W. EU road vehicle energy consumption and CO₂ emissions by 2050—Expert-based scenarios. *Energy Policy* **2020**, *138*, 111224. [[CrossRef](#)]
37. Seum, S.; Ehrenberger, S.; Pregger, T. Extended emission factors for future automotive propulsion in Germany considering fleet composition, new technologies and emissions from energy supplies. *Atmos. Environ.* **2020**, *233*, 117568. [[CrossRef](#)]
38. Olabi, A.G.; Maizak, D.; Wilberforce, T. Review of the regulations and techniques to eliminate toxic emissions from diesel engine cars. *Sci. Total Environ.* **2020**, *748*, 141249. [[CrossRef](#)] [[PubMed](#)]
39. Crippa, M.; Janssens-Maenhout, G.; Guizzardi, D.; Galmarini, S. EU effect: Exporting emission standards for vehicles through the global market economy. *J. Environ. Manag.* **2016**, *183*, 959–971. [[CrossRef](#)] [[PubMed](#)]
40. Jiménez, J.L.; Valido, J.; Molden, N. The drivers behind differences between official and actual vehicle efficiency and CO₂ emissions. *Transp. Res. Part D Transp. Environ.* **2019**, *67*, 628–641. [[CrossRef](#)]
41. Commission Regulation (EU) 2018/1832 of 5 November 2018 Amending Directive 2007/46/EC of the European Parliament and of the Council, Commission Regulation (EC) No 692/2008 and Commission Regulation (EU) 2017/1151 for the Purpose of IMPROVING the Emission Type Approval Tests and Procedures for Light Passenger and Commercial Vehicles, Including Those for In-Service Conformity and Real-Driving Emissions and Introducing Devices for Monitoring the Consumption of Fuel and Electric Energy (Text with EEA Relevance). Available online: <https://eur-lex.europa.eu/legal-content/EN/TXT/?uri=CELEX%3A32018R1832> (accessed on 1 November 2020).
42. Sun, Z.; Wen, Z.; Zhao, X.; Yang, Y.; Li, S. Real-World Driving Cycles Adaptability of Electric Vehicles. *World Electr. Veh. J.* **2020**, *11*, 19. [[CrossRef](#)]

43. Chen, L.; Wang, Z.; Liu, S.; Qu, L. Using a chassis dynamometer to determine the influencing factors for the emissions of Euro VI vehicles. *Transp. Res. Part D Transp. Environ.* **2018**, *65*, 564–573. [CrossRef]
44. Sakthivel, P.; Subramanian, K.A.; Mathai, R. Comparative studies on combustion, performance and emission characteristics of a two-wheeler with gasoline and 30% ethanol-gasoline blend using chassis dynamometer. *Appl. Therm. Eng.* **2019**, *146*, 726–737. [CrossRef]
45. Iskra, A.; Kałużny, J. Problems of Engine Tests. *Arch. Motoryz.* **2006**, *3*, 279–288.
46. Suchecki, A.; Nowakowski, J. Research during the approval process on a chassis and engine dynamometer. *TTS Tech. Transp. Szyn.* **2015**, *22*, 1459–1463.
47. Szumska, E.; Zielińska, D.; Pawełczyk, M. Construction of the Kielce Driving Cycles. *Autobusy Tech. Eksploat. Syst. Transp.* **2016**, *17*, 1372–1376.
48. Merkisz, J.; Rymaniak, Ł. Tests of urban bus specific emissions in terms of currently applicable heavy vehicles operating emission regulations. *Combust. Engines* **2017**, *168*, 21–26.
49. Mazanek, A. An overview of engine and exploitation research methods taking into account the current and future quality requirements on motor fuels. *Naft. Gaz* **2014**, *70*, 534–540.
50. Bielaczyc, P.; Szczotka, A. The potential of current European light duty CNG-fuelled vehicles to meet Euro 6 requirements. *Combust. Engines* **2012**, *4*, 20–33.
51. Technical Harmonisation in the EU. Available online: https://ec.europa.eu/growth/sectors/automotive/technical-harmonisation/eu_en (accessed on 1 November 2020).
52. Bodisco, T.; Zare, A. Practicalities and Driving Dynamics of a Real Driving Emissions (RDE) Euro 6 Regulation Homologation Test. *Energies* **2019**, *12*, 2306.
53. Moradi, E.; Miranda-Moreno, L. Vehicular fuel consumption estimation using real-world measures through cascaded machine learning modeling. *Transp. Res. Part D Transp. Environ.* **2020**, *88*, 102576. [CrossRef]
54. Chen, Y.; Gonder, J.; Young, S.; Wood, E. Quantifying autonomous vehicles national fuel consumption impacts: A data-rich approach. *Transp. Res. Part A Policy Pract.* **2019**, *122*, 134–145. [CrossRef]
55. Ma, R.; He, X.; Zheng, Y.; Zhou, B.; Lu, S.; Wu, Y. Real-world driving cycles and energy consumption informed by large-sized vehicle trajectory data. *J. Clean. Prod.* **2019**, *223*, 564–574. [CrossRef]
56. Donato, T.; Giovinazzi, M. Building a cycle for Real Driving Emissions. *Energy Procedia* **2017**, *126*, 891–898. [CrossRef]
57. Emission Test Cycles. Available online: <https://dieselnet.com/standards/cycles/index.php> (accessed on 1 November 2020).
58. Robinson, B.; Eastlake, A. Development of Test Cycles and Measurement Protocols for a Low Carbon Truck Technology Accreditation Scheme. Available online: <https://www.lowcvp.org.uk/assets/workingdocuments/Scheme%20Data%20Analysis%20Paper%20after%20Peer%20Review%20Comments%20June%202016.pdf> (accessed on 1 November 2020).
59. Merkisz, J.; Pielecha, J.; Molik, P. Analysis of vehicle working conditions in the homologation tests. *Logistyka* **2015**, *3*, 3220–3227.
60. Emissions in the Automotive Sector. Available online: https://ec.europa.eu/growth/sectors/automotive/environment-protection/emissions_en (accessed on 1 November 2020).
61. García, A.; Monsalve-Serrano, J.; Martínez-Boggio, S.; Gaillard, P.; Poussin, O.; Amer, A.A. Dual fuel combustion and hybrid electric powertrains as potential solution to achieve 2025 emissions targets in medium duty trucks sector. *Energy Convers. Manag.* **2020**, *224*, 113320.
62. Liu, Q.; Liu, J.; Fu, J.; Li, Y.; Luo, B.; Zhan, Z.; Deng, B. Comparative study on combustion and thermodynamics performance of gasoline direct injection (GDI) engine under cold start and warm-up NEDC. *Energy Convers. Manag.* **2019**, *181*, 663–673. [CrossRef]
63. Karagöz, Y. Analysis of the impact of gasoline, biogas and biogas + hydrogen fuels on emissions and vehicle performance in the WLTC and NEDC. *Int. J. Hydrog. Energy* **2019**, *44*, 31621–31632. [CrossRef]
64. Ramos, A.; Muñoz, J.; Andrés, F.; Armas, O. NOx emissions from diesel light duty vehicle tested under NEDC and real-world driving conditions. *Transp. Res. Part D Transp. Environ.* **2018**, *63*, 37–48. [CrossRef]
65. Dimaratos, A.; Tsokolis, D.; Fontaras, G.; Tsiakmakis, S.; Ciuffo, B.; Samaras, Z. Comparative Evaluation of the Effect of Various Technologies on Light-Duty Vehicle CO₂ Emissions over NEDC and WLTP. *Transp. Res. Procedia* **2016**, *14*, 3169–3178. [CrossRef]
66. Armas, O.; García-Contreras, R.; Ramos, A. On-line thermodynamic diagnosis of diesel combustion process with paraffinic fuels in a vehicle tested under NEDC. *J. Clean. Prod.* **2016**, *138*, 94–102. [CrossRef]
67. Tietge, U.; Diaz, U.; Mock, P.; German, J.; Bandivadekar, A.; Ligterink, N. From Laboratory to Road—A 2016 Update of Official and ‘Real-World’ Fuel Consumption and CO₂ Values for Passenger Cars in Europe. Available online: https://theicct.org/sites/default/files/publications/ICCT_LaboratoryToRoad_2016.pdf (accessed on 2 November 2020).
68. Pacheco, A.F.; Martins, M.E.S.; Zhao, H. New European Drive Cycle (NEDC) simulation of a passenger car with a HCCI engine: Emissions and fuel consumption results. *Fuel* **2013**, *111*, 733–739. [CrossRef]
69. Botwinska, K.; Mruk, R.; Sloma, J.; Tucki, K.; Zaleski, M. Simulation of Diesel Engine Emissions on the Example of Fiat Panda in the NEDC Test. Available online: https://www.e3s-conferences.org/articles/e3sconf/abs/2017/07/e3sconf_eems2017_02003/e3sconf_eems2017_02003.html (accessed on 1 November 2020).
70. Massaguer, E.; Massaguer, A.; Pujol, T.; Comamala, M.; Montoro, L.; Gonzalez, J.R. Fuel economy analysis under a WLTP cycle on a mid-size vehicle equipped with a thermoelectric energy recovery system. *Energy* **2019**, *179*, 306–314. [CrossRef]

71. Yu, B.; Yang, J.; Wang, D.; Shi, J.; Chen, J. Energy consumption and increased EV range evaluation through heat pump scenarios and low GWP refrigerants in the new test procedure WLTP. *Int. J. Refrig.* **2019**, *100*, 284–294. [CrossRef]
72. Tsiakmakis, S.; Fontaras, G.; Anagnostopoulos, K.; Ciuffo, B.; Pavlovic, J.; Marotta, A. A simulation based approach for quantifying CO₂ emissions of light duty vehicle fleets. A case study on WLTP introduction. *Transp. Res. Procedia* **2017**, *25*, 3898–3908.
73. Blanco-Rodriguez, D.; Vagnoni, G.; Holderbaum, B. EU6 C-Segment Diesel vehicles, a challenging segment to meet RDE and WLTP requirements. *IFAC-Pap.* **2016**, *49*, 649–656.
74. Du, B.; Zhang, L.; Geng, Y.; Zhang, Y.; Xu, H.; Xiang, G. Testing and evaluation of cold-start emissions in a real driving emissions test. *Transp. Res. Part D Transp. Environ.* **2020**, *86*, 102447. [CrossRef]
75. Wang, Y.; Hao, C.; Ge, Y.; Hao, L.; Tan, J.; Wang, X.; Zhang, P.; Wang, Y.; Tian, W.; Lin, Z.; et al. Fuel consumption and emission performance from Light-Duty conventional/hybrid-electric vehicles over different cycles and real driving tests. *Fuel* **2020**, *278*, 118340. [CrossRef]
76. Mera, Z.; Fonseca, N.; López, J.M.; Casanova, J. Analysis of the high instantaneous NOx emissions from Euro 6 diesel passenger cars under real driving conditions. *Appl. Energy* **2019**, *242*, 1074–1089. [CrossRef]
77. Suarez-Bertoa, R.; Zardini, A.A.; Keuken, H.; Astorga, C. Impact of ethanol containing gasoline blends on emissions from a flex-fuel vehicle tested over the Worldwide Harmonized Light duty Test Cycle (WLTC). *Fuel* **2015**, *143*, 173–182. [CrossRef]
78. Tutuianu, M.; Bonnel, P.; Ciuffo, B.; Haniu, T.; Ichikawa, N.; Marotta, A.; Pavlovic, J.; Steven, H. Development of the World-wide harmonized Light duty Test Cycle (WLTC) and a possible pathway for its introduction in the European legislation. *Transp. Res. Part D Transp. Environ.* **2015**, *40*, 61–75. [CrossRef]
79. Sileghem, L.; Bosteels, D.; May, J.; Favre, C.; Verhelst, S. Analysis of vehicle emission measurements on the new WLTC, the NEDC and the CADC. *Transp. Res. Part D Transp. Environ.* **2014**, *32*, 70–85.
80. Triantafyllopoulos, G.; Dimaratos, A.; Ntziachristos, L.; Bernard, Y.; Dornoff, J.; Samaras, Z. A study on the CO₂ and NOx emissions performance of Euro 6 diesel vehicles under various chassis dynamometer and on-road conditions including latest regulatory provisions. *Sci. Total Environ.* **2019**, *666*, 337–346. [CrossRef]
81. The Mobile Air-Conditioning Systems MACs. Available online: https://ec.europa.eu/growth/sectors/automotive/environment-protection/mobile-air-conditioning-systems_en (accessed on 2 November 2020).
82. Refrigerants Used in Mobile Air Condition Systems (MAC)-State of Play. Available online: https://ec.europa.eu/commission/presscorner/detail/en/MEMO_14_50 (accessed on 2 November 2020).
83. André, M.; Joumard, R.; Vidon, R.; Tassel, P.; Perret, P. Real-world European driving cycles, for measuring pollutant emissions from high- and low-powered cars. *Atmos. Environ.* **2006**, *40*, 5944–5953. [CrossRef]
84. Chindamo, D.; Gadola, M. What is the Most Representative Standard Driving Cycle to Estimate Diesel Emissions of a Light Commercial Vehicle? *IFAC-Pap.* **2018**, *51*, 73–78.
85. Benajes, J.; García, A.; Monsalve-Serrano, J.; Sari, R.L. Fuel consumption and engine-out emissions estimations of a Light-Duty engine running in dual-mode RCCI/CDC with different fuels and driving cycles. *Energy* **2018**, *157*, 19–30. [CrossRef]
86. Heinold, A. Comparing emission estimation models for rail freight transportation. *Transp. Res. Part D Transp. Environ.* **2020**, *86*, 102468. [CrossRef]
87. Di Trolio, P.; Di Giorgio, P.; Genovese, M.; Frasci, E.; Minutillo, M. A hybrid power-unit based on a passive fuel cell/battery system for lightweight vehicles. *Appl. Energy* **2020**, *279*, 115734. [CrossRef]
88. André, M. The ARTEMIS European driving cycles for measuring car pollutant emissions. *Sci. Total Environ.* **2004**, *334–335*, 73–84.
89. ARTEMIS: Assessment and Reliability of Transport Emission Models and Inventory Systems_Final Report. Available online: <http://trl.demo.varistha.co.uk/publications/ppr350> (accessed on 2 November 2020).
90. Emission Factor Modelling for Light Vehicles within the European Artemis Model. Available online: <https://core.ac.uk/download/pdf/51960921.pdf> (accessed on 2 November 2020).
91. Jenn, A.; Azevedo, I.L.; Michalek, J.J. Alternative-fuel-vehicle policy interactions increase U.S. greenhouse gas emissions. *Transp. Res. Part A Policy Pract.* **2019**, *124*, 396–407. [CrossRef]
92. Kang, S.; Min, K. Dynamic simulation of a fuel cell hybrid vehicle during the federal test procedure-75 driving cycle. *Appl. Energy* **2016**, *161*, 181–196. [CrossRef]
93. Xue, J.; Li, Y.; Quiros, D.; Hu, S.; Huai, T.; Ayala, A.; Jung, H.S. Investigation of alternative metrics to quantify PM mass emissions from light duty vehicles. *J. Aerosol. Sci.* **2017**, *113*, 85–94. [CrossRef]
94. Xue, J.; Johnson, K.; Durbin, T.; Russell, R.; Pham, L.; Miller, W.; Swanson, J.; Kittelson, D.; Jung, H. Very low particle matter mass measurements from Light-Duty vehicles. *J. Aerosol. Sci.* **2018**, *117*, 1–10. [CrossRef]
95. Borlaug, B.; Holden, J.; Wood, E.; Lee, B.; Fink, J.; Agnew, S.; Lustbader, J. Estimating region-specific fuel economy in the United States from real-world driving cycles. *Transp. Res. Part D Transp. Environ.* **2020**, *86*, 102448. [CrossRef]
96. Kim, J.; Choi, K.; Myung, C.L.; Lee, Y.; Park, S. Comparative investigation of regulated emissions and nano-particle characteristics of light duty vehicles using various fuels for the FTP-75 and the NEDC mode. *Fuel* **2013**, *106*, 335–343. [CrossRef]
97. Kim, J.; Kim, K.; Oh, S. An assessment of the ultra-lean combustion direct-injection LPG (liquefied petroleum gas) engine for passenger-car applications under the FTP-75 mode. *Fuel Process. Technol.* **2016**, *154*, 219–226. [CrossRef]
98. Arvajová, A.; Kočí, P. Impact of PtOx formation in diesel oxidation catalyst on NO₂ yield during driving cycles. *Chem. Eng. Sci.* **2017**, *158*, 181–187. [CrossRef]

99. Khan, T.; Frey, H.C. Comparison of real-world and certification emission rates for light duty gasoline vehicles. *Sci. Total Environ.* **2018**, *622–623*, 790–800. [CrossRef] [PubMed]
100. Myung, C.L.; Jang, W.; Kwon, S.; Ko, J.; Jin, D.; Park, S. Evaluation of the real-time de-NO_x performance characteristics of a LNT-equipped Euro-6 diesel passenger car with various vehicle emissions certification cycles. *Energy* **2017**, *132*, 356–369. [CrossRef]
101. Huai, T.; Durbin, T.D.; Miller, J.W.; Norbeck, J.M. Estimates of the emission rates of nitrous oxide from Light-Duty vehicles using different chassis dynamometer test cycles. *Atmos. Environ.* **2004**, *38*, 6621–6629. [CrossRef]
102. Borsari, V.; De Assunção, J.V. Ammonia emissions from a Light-Duty vehicle. *Transp. Res. Part D Transp. Environ.* **2017**, *51*, 53–61. [CrossRef]
103. Karabasoglu, O.; Michalek, J. Influence of driving patterns on life cycle cost and emissions of hybrid and plug-in electric vehicle powertrains. *Energy Policy* **2013**, *60*, 445–461. [CrossRef]
104. Myung, C.L.; Kim, J.; Choi, K.; Hwang, I.G.; Park, S. Comparative study of engine control strategies for particulate emissions from direct injection Light-Duty vehicle fueled with gasoline and liquid phase liquefied petroleum gas (LPG). *Fuel* **2012**, *94*, 348–355. [CrossRef]
105. Cho, C.P.; Kwon, O.S.; Lee, Y.L. Effects of the sulfur content of liquefied petroleum gas on regulated and unregulated emissions from liquefied petroleum gas vehicle. *Fuel* **2014**, *137*, 328–334. [CrossRef]
106. European Cars Emit more CO₂. Among the Guilty SUVs. Available online: <https://biznes.autokult.pl/33260,europejskie-samochody-emituja-wiecej-co2-wsrod-winnych-suv-y> (accessed on 5 November 2020).
107. New CO₂ Standards will Change the Automotive Industry. Available online: <https://kaizenfleet.pl/nowe-normy-co2-odmienia-branze-motoryzacyjna/> (accessed on 5 November 2020).
108. More than €14. 5 Billion-That's What the EU can Earn from Car Manufacturers. Available online: <https://moto.rp.pl/tu-i-teraz/38317-ponad-145-mlrd-euro-tyle-ue-moze-zarobic-na-producentach-samochodow> (accessed on 5 November 2020).
109. Wasiak, A. *Modeling Energetic Efficiency of Biofuels Production*. *Green Energy and Technology*, 1st ed.; Springer Nature Switzerland: Cham, Switzerland, 2018; pp. 29–47, ISBN 978-3-319-98430-8. [CrossRef]
110. Javed, S.A.; Zhu, B.; Liu, S. Forecast of biofuel production and consumption in top CO₂ emitting countries using a novel grey model. *J. Clean. Prod.* **2020**, *276*, 123997. [CrossRef]
111. Will the “Green” Diesel Help to Solve Problems with RES in Transport? Available online: <https://wysokienapiecie.pl/18240-biopaliwa-w-transporcie-przejda-zmiany-po-2020-r/> (accessed on 5 November 2020).
112. Mikulski, M.; Ambrosewicz-Walacik, M.; Duda, K.; Hunicz, J. Performance and emission characterization of a common-rail compression-ignition engine fuelled with ternary mixtures of rapeseed oil, pyrolytic oil and diesel. *Renew. Energy* **2020**, *148*, 739–755. [CrossRef]
113. Bemani, A.; Xiong, Q.; Baghban, A.; Habibzadeh, S.; Mohammadi, A.H.; Doranehgard, M.H. Modeling of cetane number of biodiesel from fatty acid methyl ester (FAME) information using GA-, PSO-, and HGAPSO- LSSVM models. *Renew. Energy* **2020**, *150*, 924–934. [CrossRef]
114. Alves-Fortunato, M.; Ayoub, E.; Bacha, K.; Mouret, A.; Dalmazzone, C. Fatty Acids Methyl Esters (FAME) autoxidation: New insights on insoluble deposit formation process in biofuels. *Fuel* **2020**, *268*, 117074. [CrossRef]
115. Bharathiraja, B.; Jayamuthunagai, J.; Sudharsanaa, T.; Bharghavi, A.; Praveenkumar, R.; Chakravarthy, M.; Yuvaraj, D. Biobutanol—An impending biofuel for future: A review on upstream and downstream processing techniques. *Renew. Sustain. Energy Rev.* **2017**, *68*, 788–807. [CrossRef]
116. Tsai, T.Y.; Lo, Y.C.; Dong, C.D.; Nagarajan, D.; Chang, J.S.; Lee, D.J. Biobutanol production from lignocellulosic biomass using immobilized *Clostridium acetobutylicum*. *Appl. Energy* **2020**, *277*, 115531. [CrossRef]
117. Lin, C.Y.; Lu, C. Development perspectives of promising lignocellulose feedstocks for production of advanced generation biofuels: A Review. *Renew. Sustain. Energy Rev.* **2021**, *136*, 110445. [CrossRef]
118. Ananthi, V.; Raja, R.; Carvalho, I.S.; Brindhadevi, K.; Pugazhendhi, A.; Arun, A. A realistic scenario on microalgae based biodiesel production: Third generation biofuel. *Fuel* **2021**, *284*, 118965. [CrossRef]
119. European Funded Project Results: Reduction of CO₂ Emissions from Heavy-Duty Trucks. Available online: <https://www.transportmeasures.org/wp-content/uploads/2017/11/VECTO-COM-Dimitrios-Savvidis-presentation.pdf> (accessed on 8 December 2020).
120. Fontaras, G.; Grigoratos, T.; Savvidis, D.; Anagnostopoulos, K.; Luz, R.; Rexeis, M.; Hausberger, S. An experimental evaluation of the methodology proposed for the monitoring and certification of CO₂ emissions from heavy-duty vehicles in Europe. *Energy* **2016**, *102*, 354–364. [CrossRef]
121. López-Martínez, J.M.; Jiménez, F.; Páez-Ayuso, F.J.; Flores-Holgado, M.N.; Arenas, A.N.; Arenas-Ramirez, B.; Aparicio-Izquierdo, F. Modelling the fuel consumption and pollutant emissions of the urban bus fleet of the city of Madrid. *Transp. Res. Part D Transp. Environ.* **2017**, *52*, 112–127. [CrossRef]
122. Mata, C.; De Oliveira Leite, W.; Moreno, R.; Agudelo, J.R.; Armas, O. Prediction of NO_x Emissions and Fuel Consumption of a City Bus under Real Operating Conditions by Means of Biharmonic Maps. *J. Energy Eng.* **2016**, *142*, 04016018. [CrossRef]
123. United Nations Economic Commission for Europe. Gearshift Calculation Tool. Available online: <https://wiki.unece.org/display/trans/Gearshift+calculation+tool> (accessed on 5 November 2020).

124. Kordylewski, W. *Spalanie i Paliwa*, 5th ed.; Oficyna Wydawnicza Politechniki Wrocławskiej: Wrocław, Poland, 2008; pp. 10–470, ISBN 978-83-7493-378-0.
125. Baczewski, K.; Kałdoński, T. *Paliwa Do Silników O Zapłonie Samoczynnym*, 2nd ed.; Wydawnictwa Komunikacji i Łączności: Warszawa, Polska, 2017; pp. 50–210.
126. Gwardiak, H.; Rozycki, K.; Ruskarska, M.; Tylus, J.; Walisiewicz-Niedbalska, W. Evaluation of fatty acid methyl esters (FAME) obtained from various feedstock. *Rosliny Oleiste Oilseed Crop*. **2011**, *32*, 137–147.
127. 2013 Mercedes E350 BlueTEC Vehicle Diesel Fuel—Test Data Package. Version 2018-09. Ann Arbor, MI: US EPA, National Vehicle and Fuel Emissions Laboratory, National Center for Advanced Technology. 2018. Available online: <https://www.epa.gov/vehicle-and-fuel-emissions-testing/benchmarking-advanced-low-emission-Light-Duty-vehicle-technology> (accessed on 5 November 2020).
128. Automobile Catalog. 2013 Mercedes-Benz E 350. Available online: https://www.automobile-catalog.com/car/2013/1553585/mercedes-benz_e_350_cdi_4matic_blueefficiency_7g-tronic.html (accessed on 5 November 2020).
129. Scilab 6.1.0. Available online: <https://www.scilab.org/> (accessed on 5 November 2020).
130. ATOMS: Neural Network Module. Available online: <http://atoms.scilab.org/toolboxes/neuralnetwork/3.0> (accessed on 5 November 2020).
131. SFTP Cycle Contributionsto Light-Duty Diesel Exhaust Emissions. Available online: <https://apps.dtic.mil/dtic/tr/fulltext/u2/a402903.pdf> (accessed on 5 November 2020).
132. Californias Advanced Clean Cars Midterm Review. Available online: https://ww2.arb.ca.gov/sites/default/files/2020-01/appendix_k_pm_test_results_ac.pdf (accessed on 5 November 2020).
133. EPA Highway Fuel Economy Test Cycle (HWFET). Available online: <https://dieselnet.com/standards/cycles/hwfet.php> (accessed on 5 November 2020).
134. Development of Test Cycle Conversion Factors among Worldwide Light-Duty Vehicle CO₂ Emission Standards. Available online: https://theicct.org/sites/default/files/publications/ICCT_LDV-test-cycle-conversion-factors_sept2014.pdf (accessed on 5 November 2020).
135. Maricq, M.M.; Szente, J.J.; Harwell, A.L.; Loos, M.J. Impact of aggressive drive cycles on motor vehicle exhaust PM emissions. *J. Aerosol. Sci.* **2017**, *113*, 1–11. [[CrossRef](#)]
136. Light-Duty Alternative Fuel Vehicles: Federal Test Procedure Emissions Results. Available online: <https://core.ac.uk/download/pdf/193176398.pdf> (accessed on 5 November 2020).
137. Ko, J.; Jin, D.; Jang, W.; Myung, C.L.; Kwon, S.; Park, S. Comparative investigation of NO_x emission characteristics from a Euro 6-compliant diesel passenger car over the NEDC and WLTC at various ambient temperatures. *Appl. Energy* **2017**, *187*, 652–662. [[CrossRef](#)]
138. Bermúdez, V.; Lujan, J.M.; Pla, B.; Linares, W.G. Comparative study of regulated and unregulated gaseous emissions during NEDC in a Light-Duty diesel engine fuelled with Fischer Tropsch and biodiesel fuels. *Biomass Bioenergy* **2011**, *35*, 789–798. [[CrossRef](#)]
139. Exhaust Emission Test Procedure for SC03 Emissions. Available online: <https://www.law.cornell.edu/cfr/text/40/86.160-00> (accessed on 7 November 2020).
140. Staff Report. Public Hearing to Consider Adoption of New Certification Tests and Standards to Control Exhaust Emissions from Aggressive Driving and Air-Conditioner Usage for Passenger Cars, Light-Duty Trucks, and Medium-Duty Vehicles under 8501 Pounds Gross Vehicle Weight Rating. Available online: <https://ww3.arb.ca.gov/regact/offcycle/staffrep.pdf> (accessed on 7 November 2020).
141. Kooijman, D.G.; Balau, A.E.; Wilkins, S.; Ligterink, N.; Cuelenaere, R. WLTP Random Cycle Generator. In Proceedings of the 12th IEEE Vehicle Power and Propulsion Conference (VPPC 2015), Montreal, QC, Canada, 19–22 October 2015.
142. May, J.; Favre, C.; Bosteels, D.; Andersson, J.; Clarke, D.; Heaney, M. On-Road Testing and PEMS Data Analysis for Two Euro 6 Diesel Vehicles. Available online: <http://www.aecc.eu/wp-content/uploads/2016/08/140918-AECC-paper-on-RDE-TAP-Conference-Graz.pdf> (accessed on 7 November 2020).
143. Random Cycle Generator. Available online: <https://www.tno.nl/en/focus-areas/traffic-transport/roadmaps/sustainable-traffic-and-transport/sustainable-mobility-and-logistics/improving-air-quality-by-monitoring-real-world-emissions/random-cycle-generator/> (accessed on 7 November 2020).
144. RTS 95 Cycle. Available online: <https://dieselnet.com/standards/cycles/rts95.php> (accessed on 7 November 2020).
145. MAC Test Procedure to be Used in a Pilot Phase. Available online: <https://www.unece.org/fileadmin/DAM/trans/doc/2011/wp29grpe/ECE-TRANS-WP29-GRPE-61-inf21e.pdf> (accessed on 7 November 2020).
146. Common Artemis Driving Cycles (CADC). Available online: <https://dieselnet.com/standards/cycles/artemis.php> (accessed on 7 November 2020).
147. EU: Light-Duty: Artemis. Available online: <https://www.transportpolicy.net/standard/eu-Light-Duty-artemis/> (accessed on 7 November 2020).
148. Zachiotis, A.T.; Giakoumis, E.G. Non-regulatory parameters effect on consumption and emissions from a diesel-powered van over the WLTC. *Transp. Res. Part D Transp. Environ.* **2019**, *74*, 104–123. [[CrossRef](#)]